

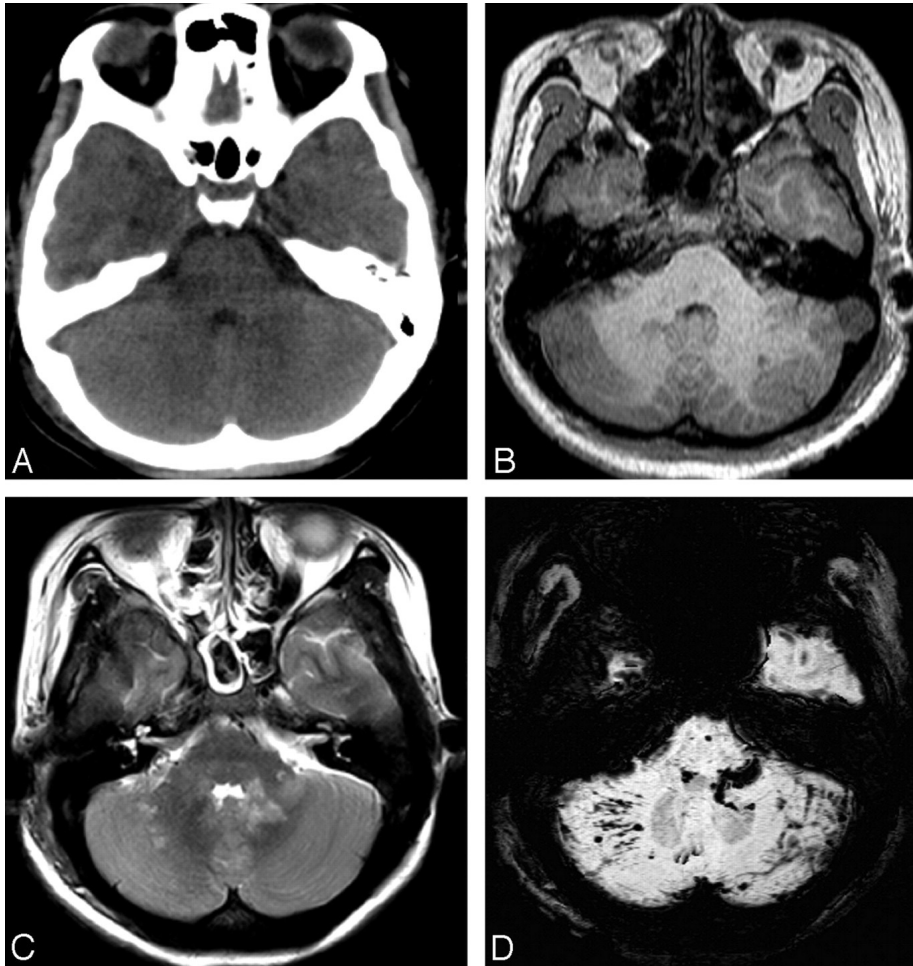
# Susceptibility MRI

Jingwen Yao, Ph.D.  
May 29, 2025

**UCLA**

**David Geffen School of Medicine**

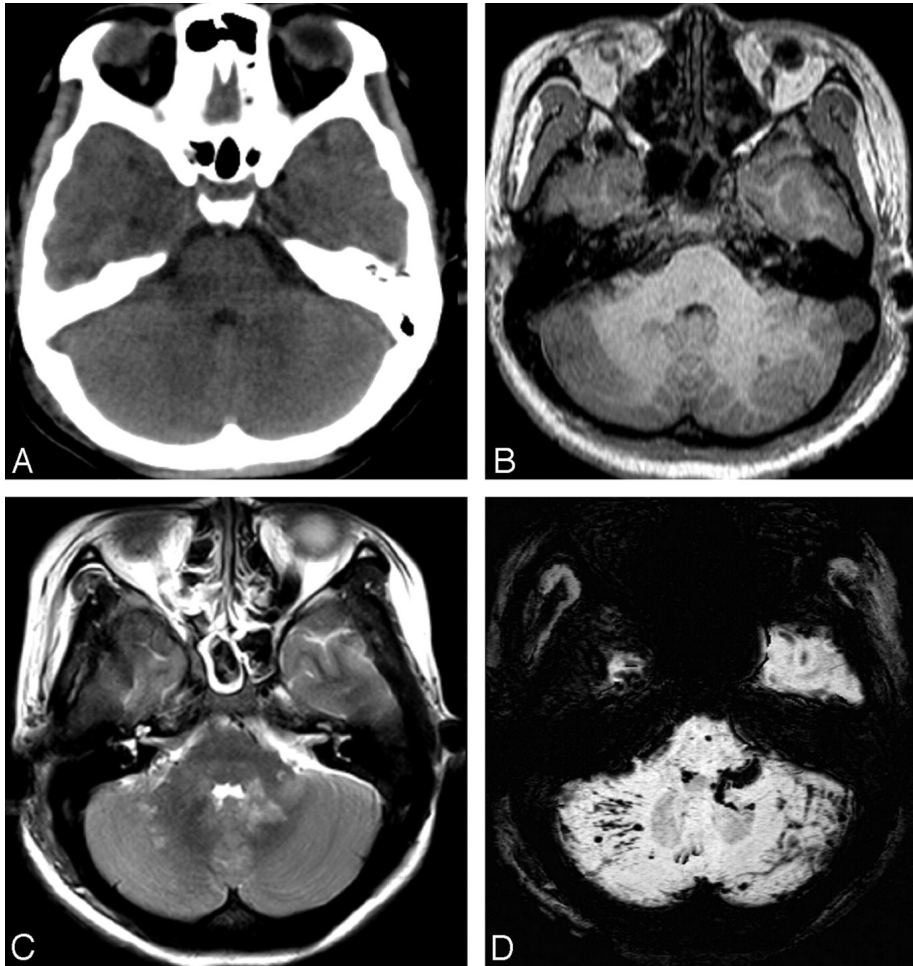
**UCLA** **Samueli**  
School of Engineering



- 38 years old woman
- Involved in a **motor vehicle crash** and sustained severe head injuries resulting in a **coma**
- CT and MR images obtained on the second day of hospitalization

#### SWI

- Striking hypointense lesions in the left brachium pontis and both hemispheres of the cerebellum
- Greater number and larger size of lesions compared with other conventional sequences



- 38 years old woman
- Involved in a **motor vehicle crash** and sustained severe head injuries resulting in a **coma**
- CT and MR images obtained on the second day of hospitalization

## Diagnosis: Diffuse axonal injury



**What is the origin of the hypointense lesions on SWI**

Paramagnetic deoxygenated blood products

# Outline

Phase in MRI

Susceptibility MRI Contrast

Susceptibility MRI Processing

Susceptibility-weighted imaging (SWI)

Quantitative susceptibility mapping (QSM)

Susceptibility MRI Applications

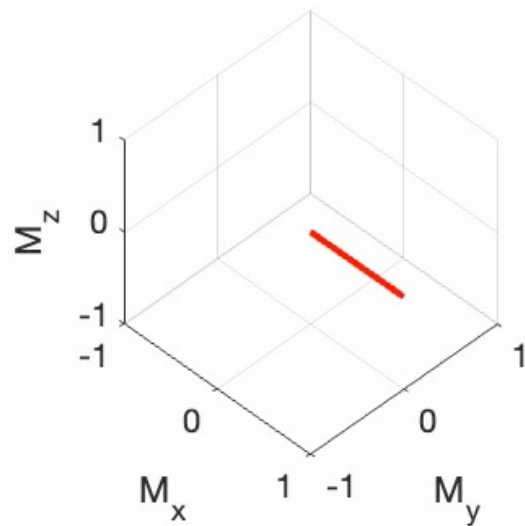
## Learning Objectives

- Explain the biological and physical basis of susceptibility effects in MRI.
- Interpret and process phase images for SWI.
- Understand the procedure of processing QSM.
- Recognize common applications of susceptibility imaging in neuroimaging.
- Appreciate the challenges and assumptions in going from phase to susceptibility maps.

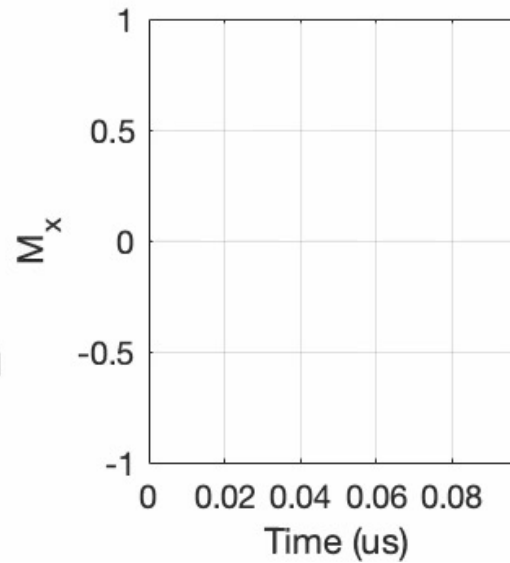


# Phase in MRI

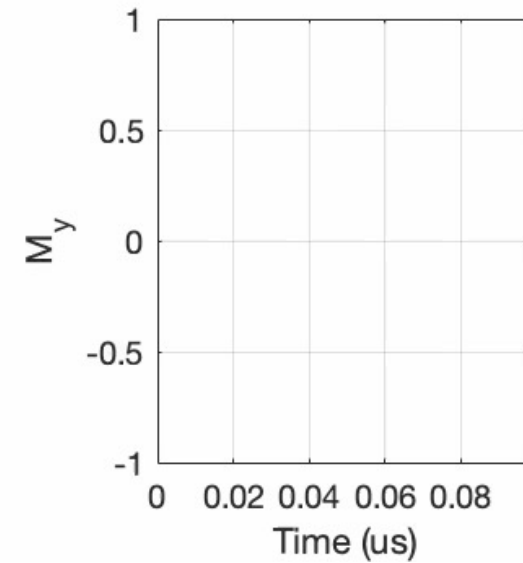
Precession of Magnetization



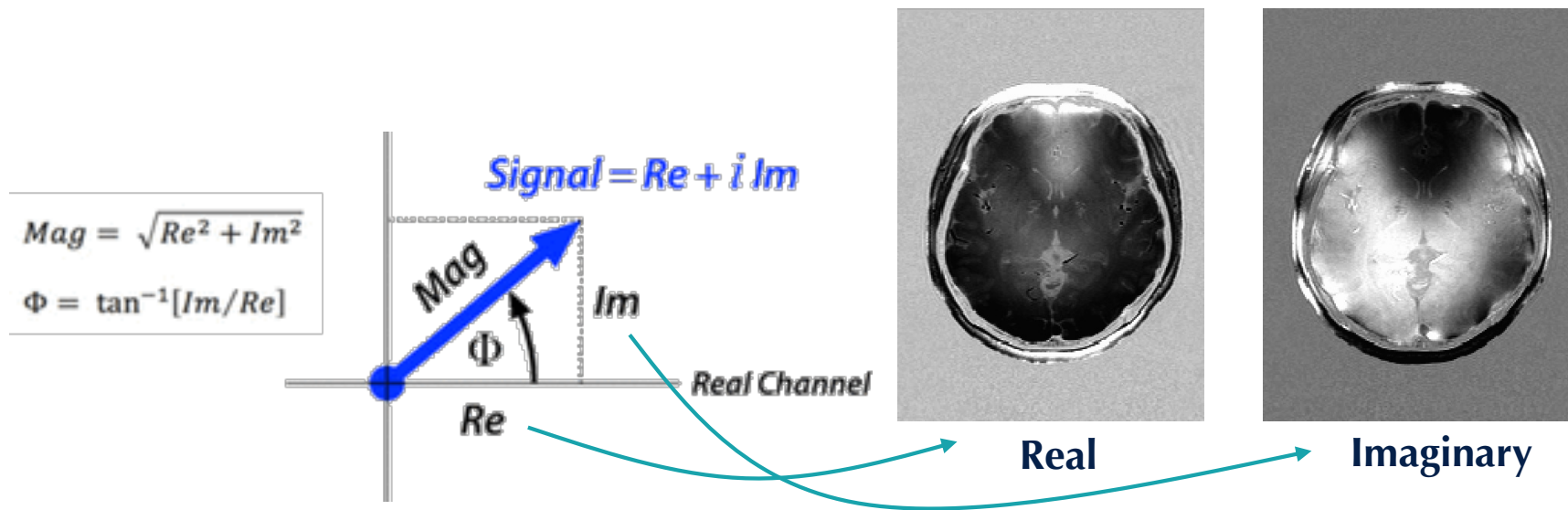
Real



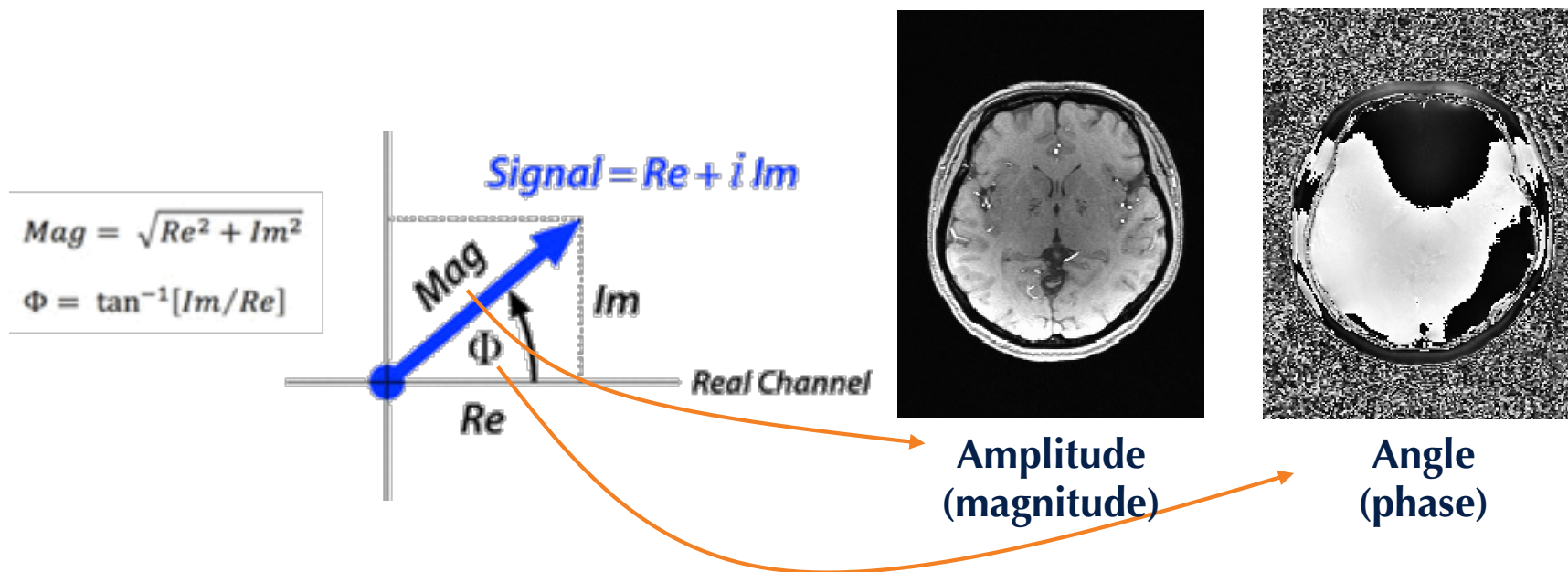
Imaginary



# Phase in MRI



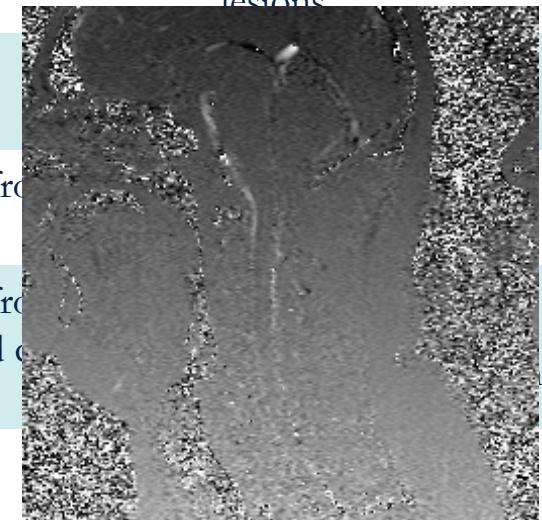
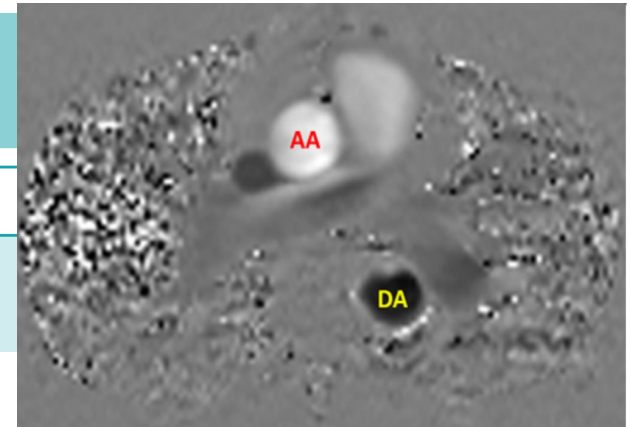
# Phase in MRI



# Phase MRI

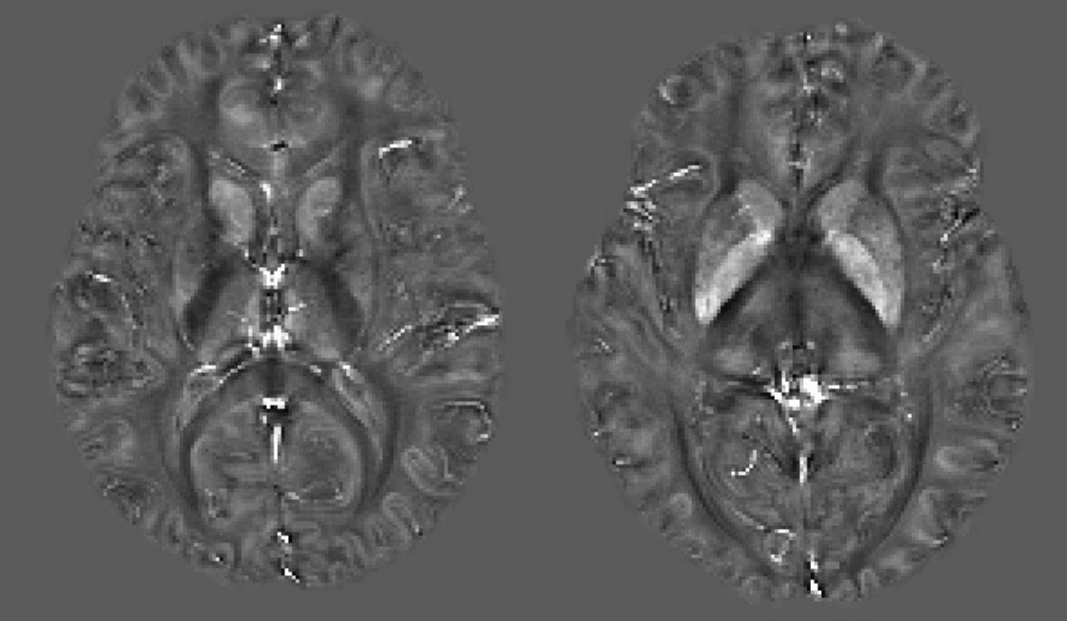
	Encoding	Data	Applications
Susceptibility imaging	None	Raw phase	Iron, calcium, myelin imaging
Conductivity imaging	None / External current	Raw phase ( $B_1$ )	Tumors, ischemic lesions
MR thermometry	None	Phase shift	MR-guided procedures
Flow imaging	Velocity-encoding bipolar gradient	Subtracted phase data from opposite encodings	Cardiac flow, CSF flow
Phase contrast angiography	Bipolar gradients applied along the x, y, and z axes sequentially	Subtracted phase data from opposite encodings and combined across three directions	Angiogram, venogram, aneurysm
Elastography	Motion-encoding gradients	Phase differences	Liver fibrosis, brain

# Phase MRI



	Encoding	Data
Susceptibility imaging	None	Raw phase
Conductivity imaging	None / External current	Raw phase ( $B_1$ )
MR thermometry	None	Phase shift
Flow imaging	Velocity-encoding bipolar gradient	Subtracted phase data from opposite encodings
Phase contrast angiography	Bipolar gradients applied along the x, y, and z axes sequentially	Subtracted phase data from opposite encodings and across three directions
Elastography	Motion-encoding gradients	Phase differences

# Phase MRI

	Encoding	Data	Applications
Susceptibility imaging	None	Raw phase	Iron, calcium, myelin imaging
Conductivity imaging	None / External current		
MR thermometry	None		
Flow imaging	Velocity-encoding bipolar gradient		
Phase contrast angiography	Bipolar gradients applied along the x and z axes sequentially		
Elastography	Motion-encoding gradients		

# Susceptibility MRI – source of contrast

## Magnetic Field H

Externally applied “magnetizing force”

Independent of medium

A/m

## Magnetic Flux Density B

(also referred to as magnetic field in MRI)

Actual magnetic field induced

Dependent of medium  
(M/J): intrinsic magnetization)

Tesla

$$B = \mu_0(H + M) = \mu_0 H + J$$

$\mu_0$ :  $4 \cdot \pi \cdot 10^{-7}$  (H/m) is the permeability of vacuum



## Susceptibility MRI – source of contrast



**Which of the statements about H and B are correct?**

- A. In an empty scanner, H and B are equivalent.
- B. The difference between B and H is due to the material's magnetization.
- C. H and B always point in the same direction.
- D. B is always stronger than H.

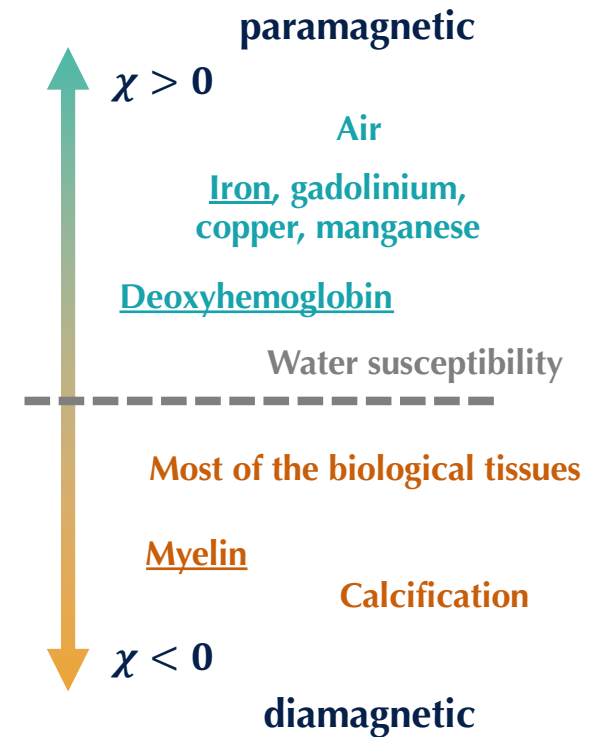
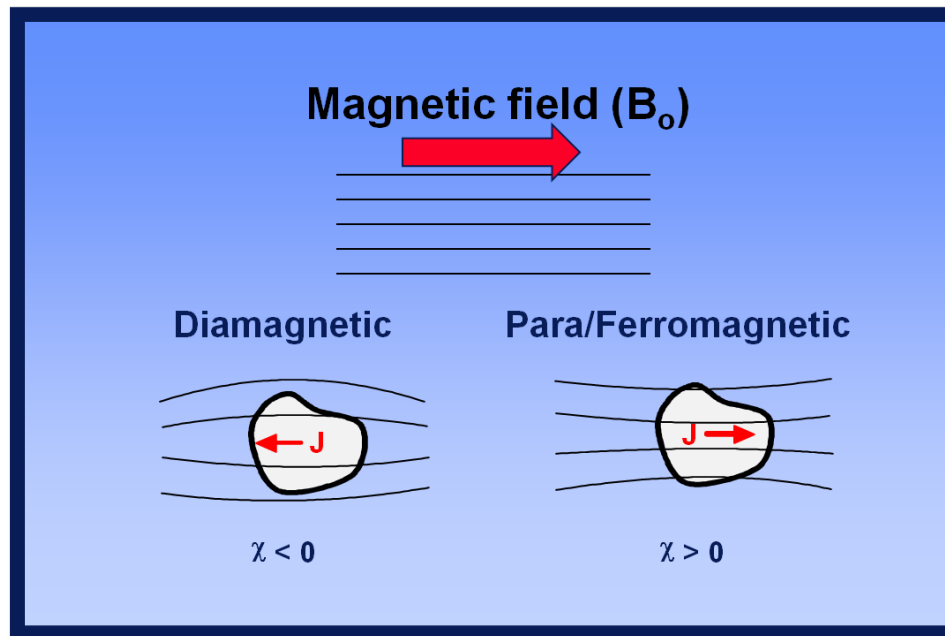


[PollEv.com/smoothdove577](https://PollEv.com/smoothdove577)

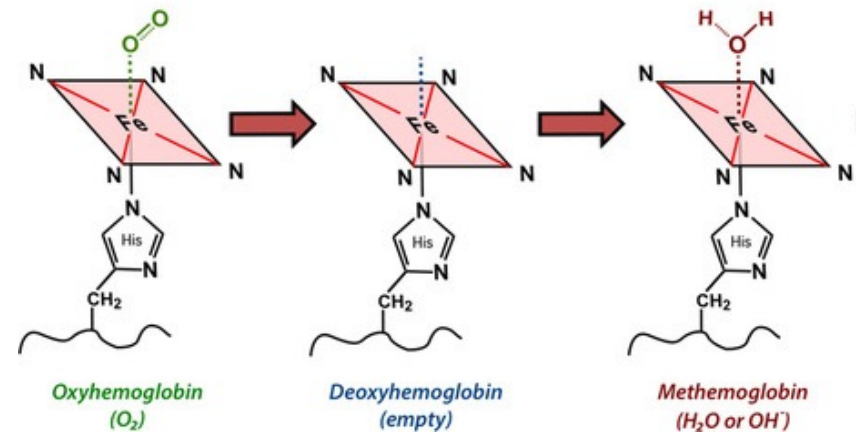
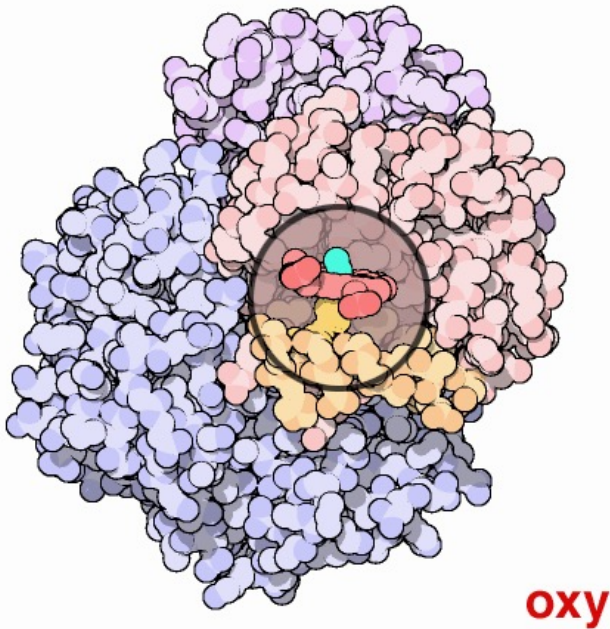
# Susceptibility MRI – source of contrast

$$B = \mu_0(H + M) = \mu_0H + J = B_0 + J$$

$$J = \chi B_0$$

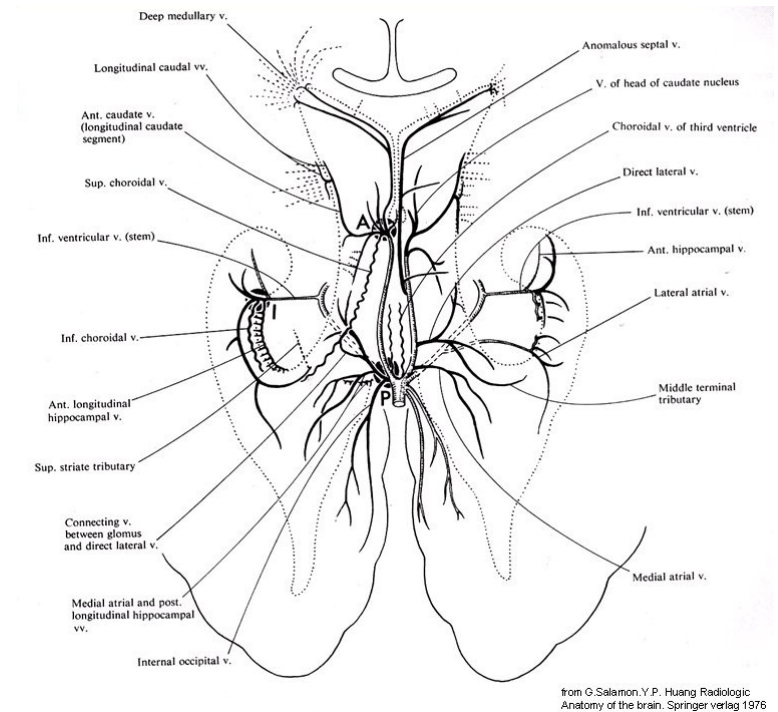
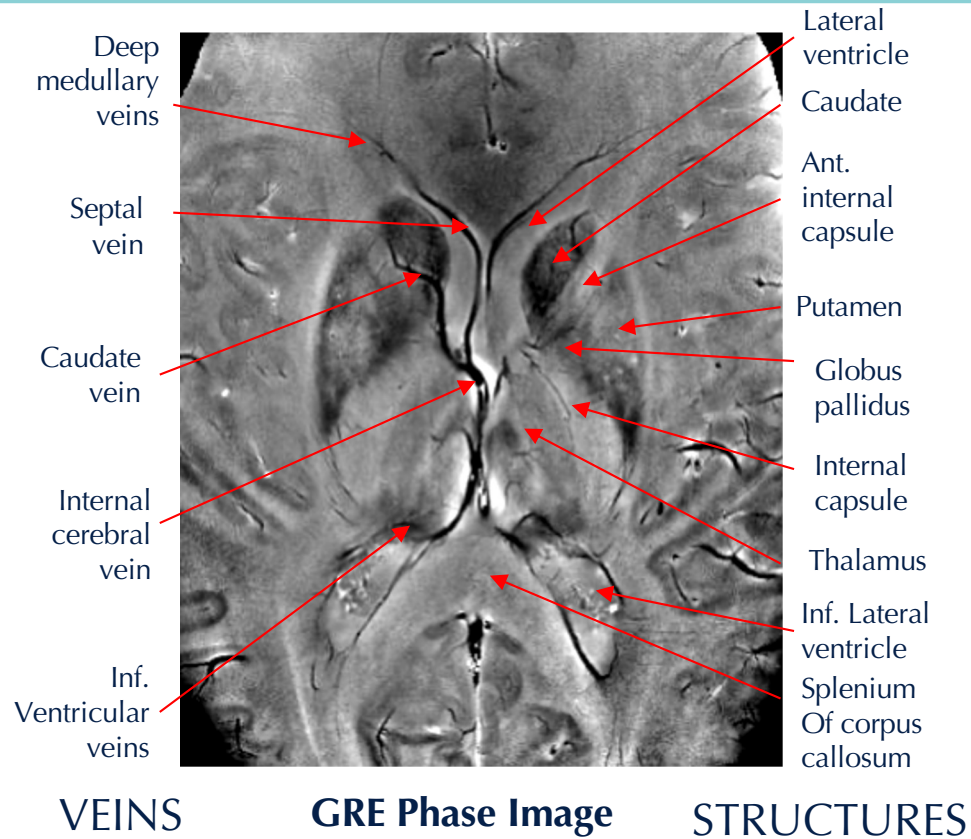


# Susceptibility MRI – source of contrast

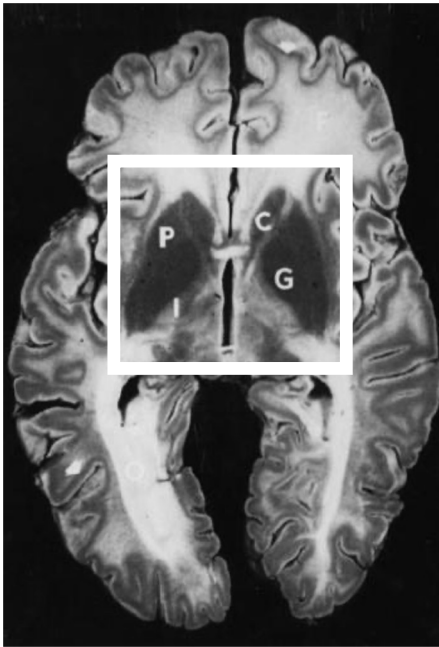


# Unpaired electrons	0	4	5
Magnetic susceptibility	Diamagnetic $\chi < 0$	Paramagnetic $\chi > 0$	Paramagnetic $\chi > 0$

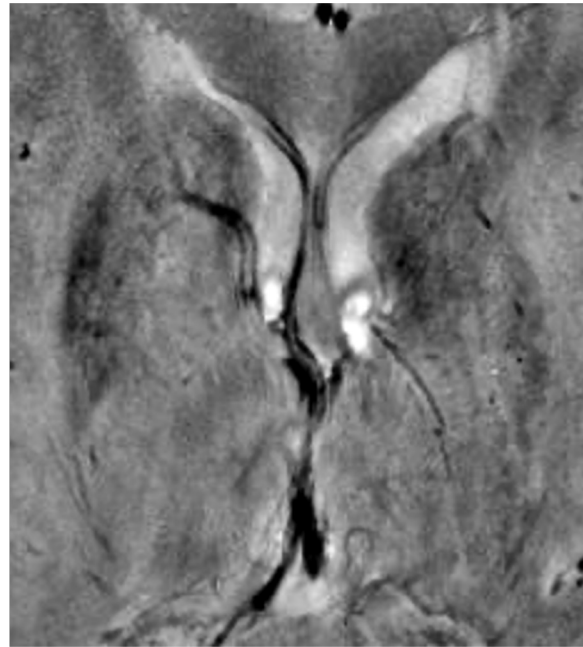
# Susceptibility MRI – Deoxyhemoglobin



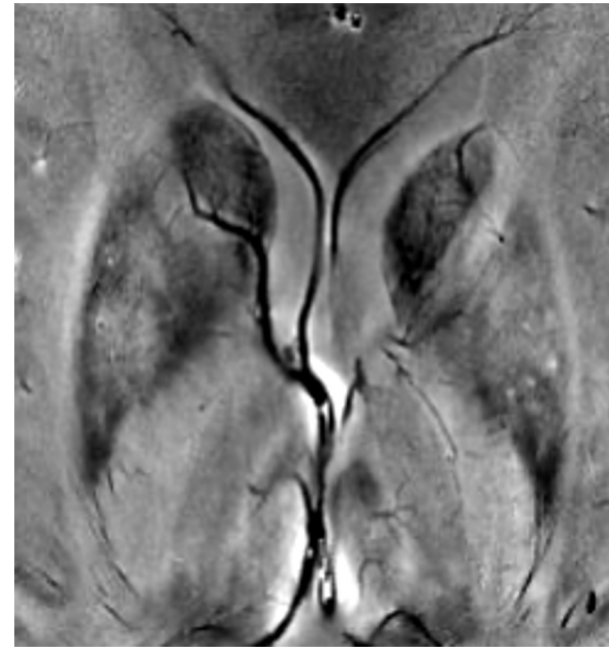
## Susceptibility MRI – Iron



**Iron Perl's Stain**

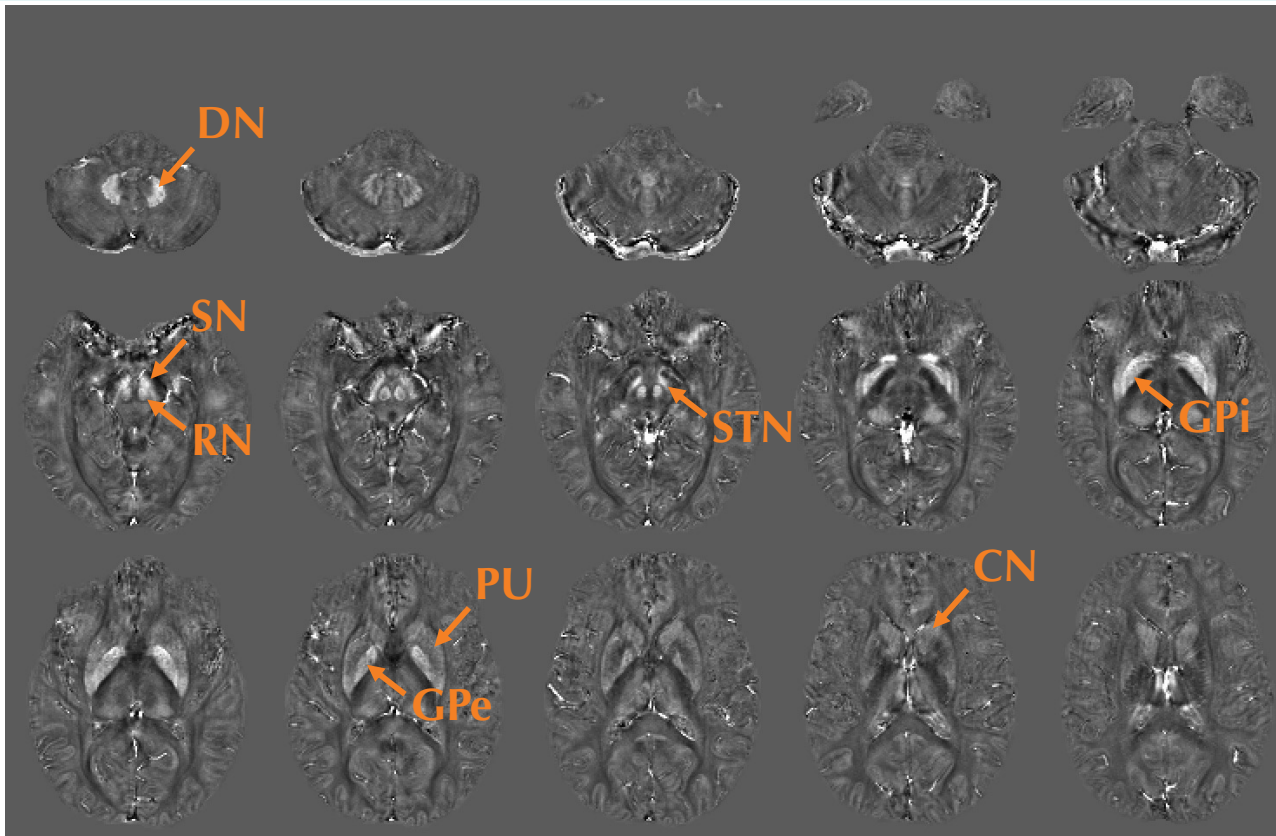


**GRE Magnitude Image**



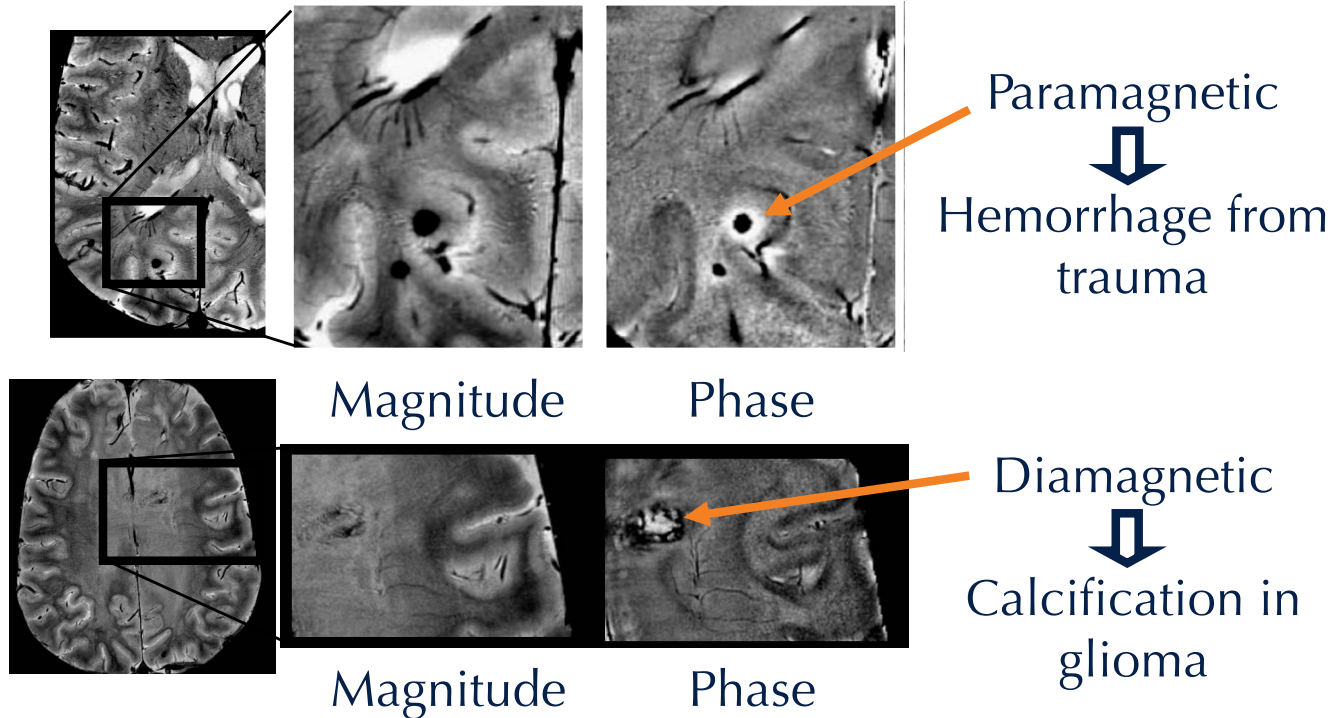
**GRE Phase Image**

## Susceptibility MRI – Iron





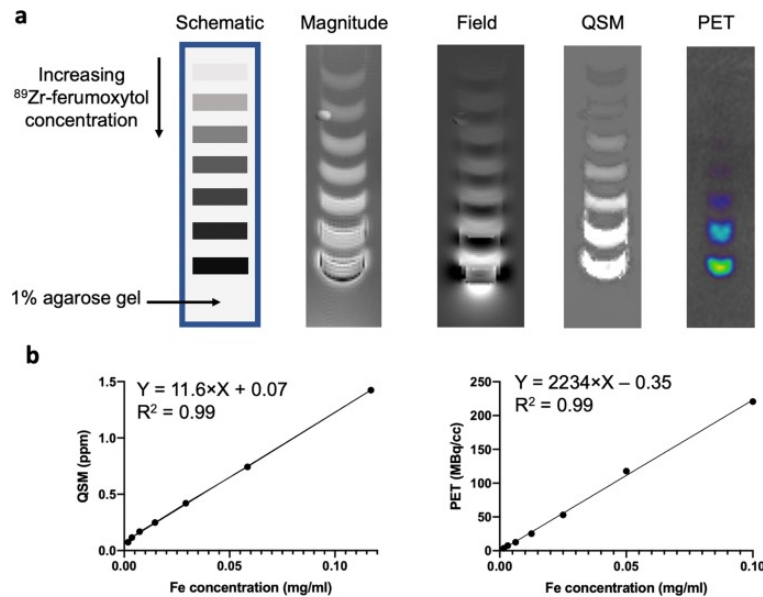
## Susceptibility MRI – Calcification



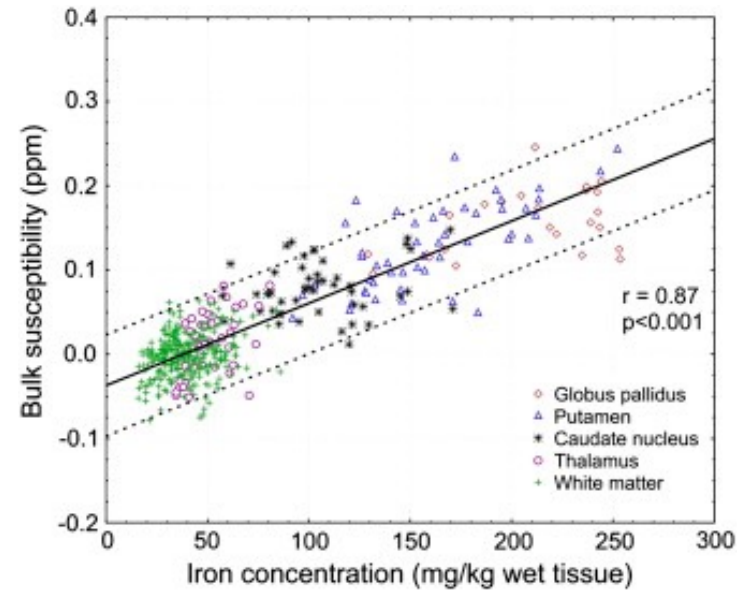


# Susceptibility MRI – Iron

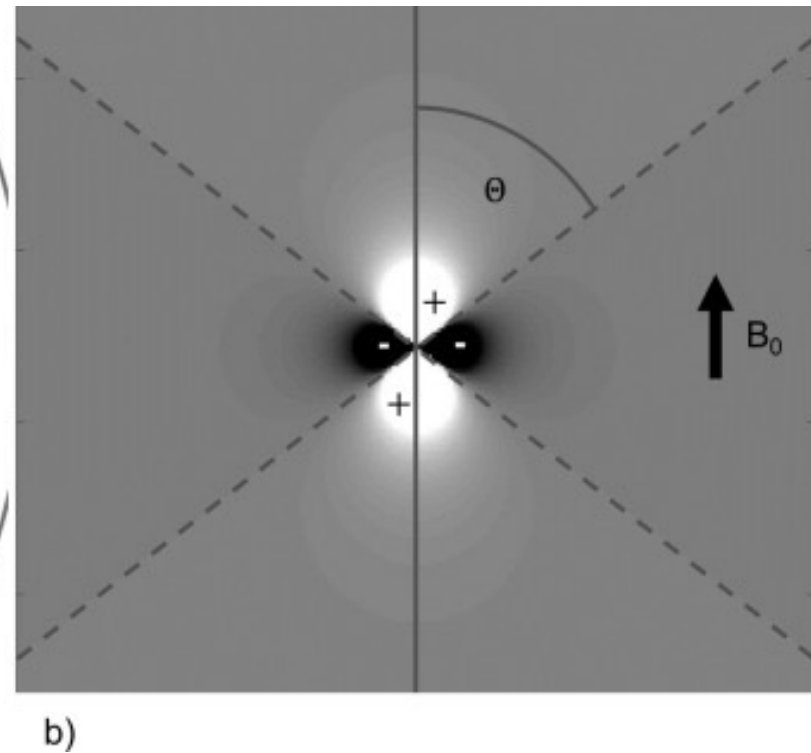
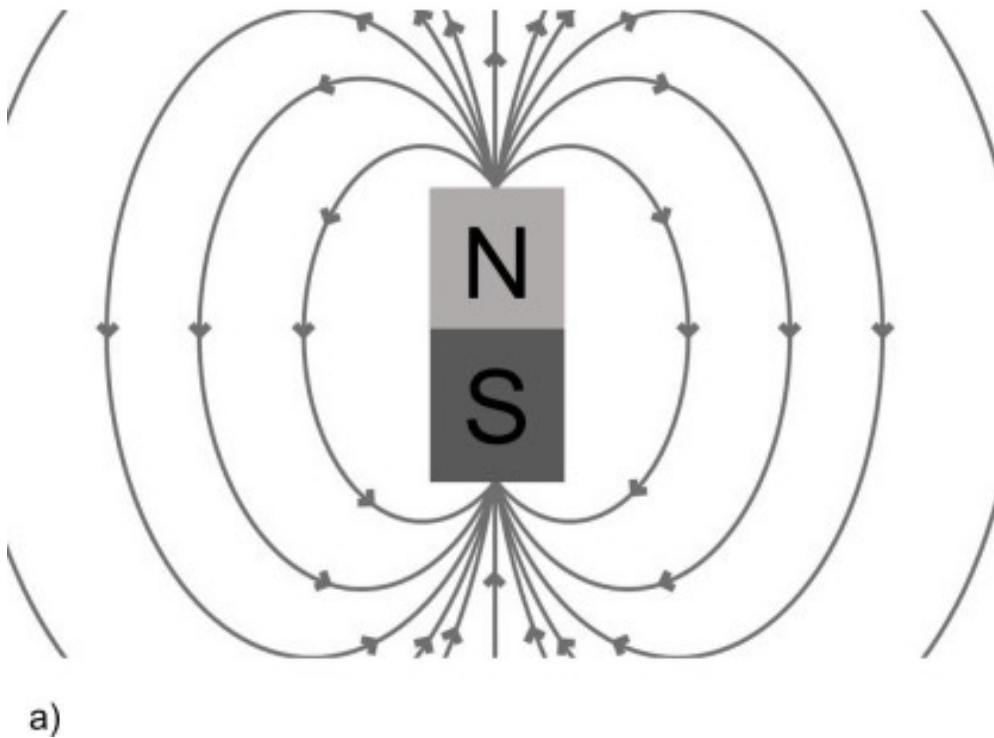
## Phantom validation



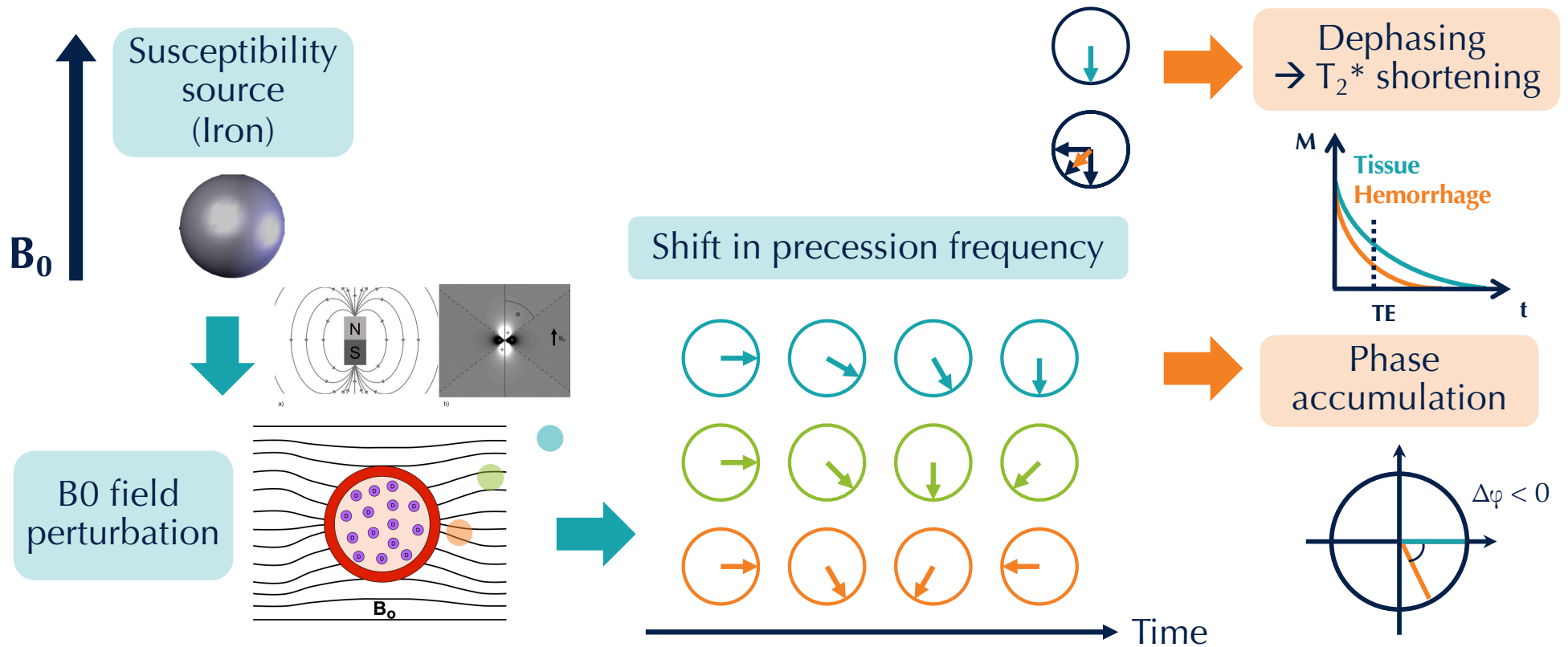
## Tissue validation



## Susceptibility MRI – Signal model

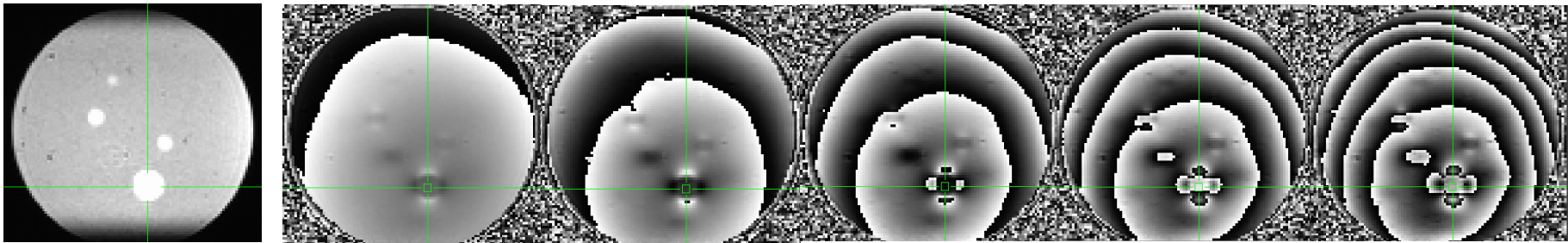


# Susceptibility MRI – MR signal



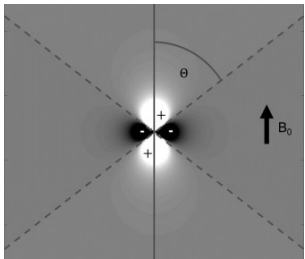
# Susceptibility MRI – Signal model

Ferumoxytol phantom



5.84 ms

40.56 ms



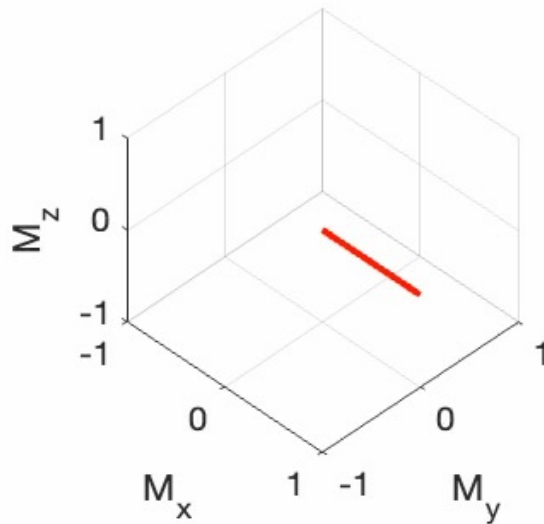
Where does the phase discontinuity come from?



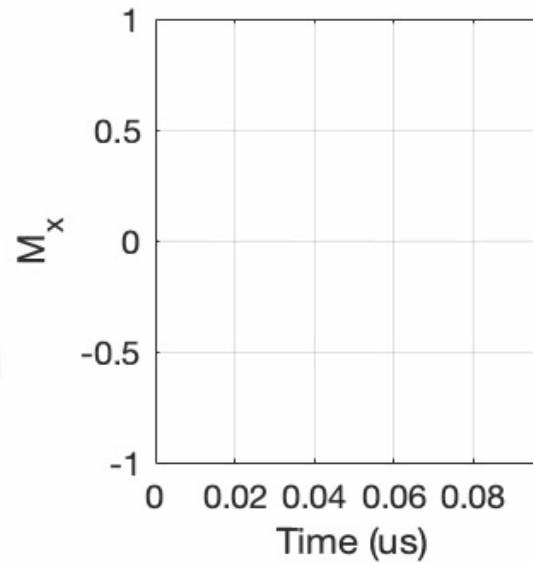
[PollEv.com/smoothdove577](https://PollEv.com/smoothdove577)

# Susceptibility MRI – Signal model

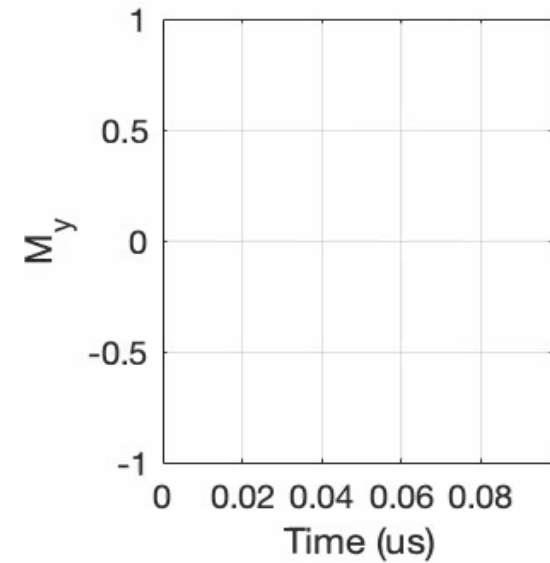
Precession of Magnetization



Real

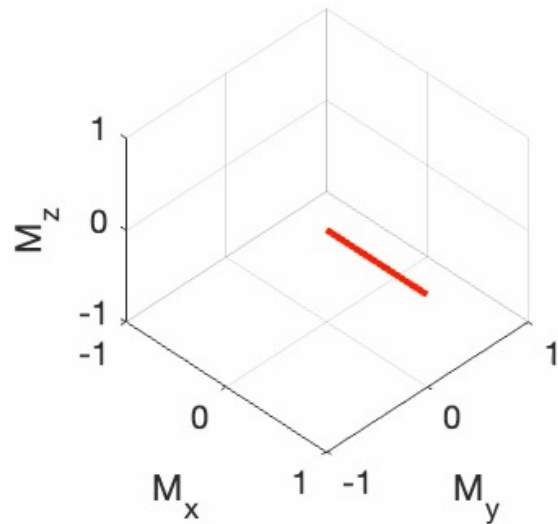


Imaginary

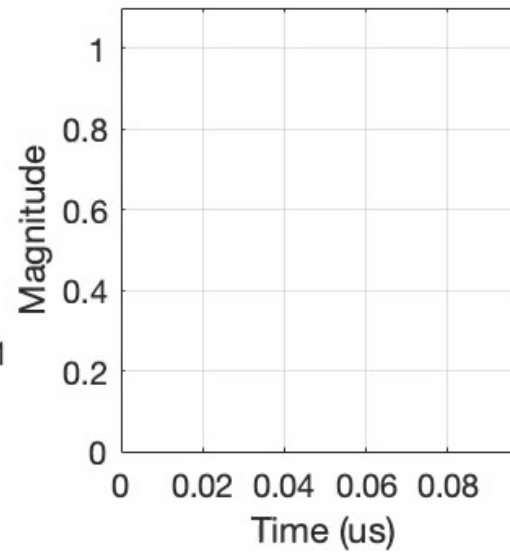


# Susceptibility MRI – Signal model

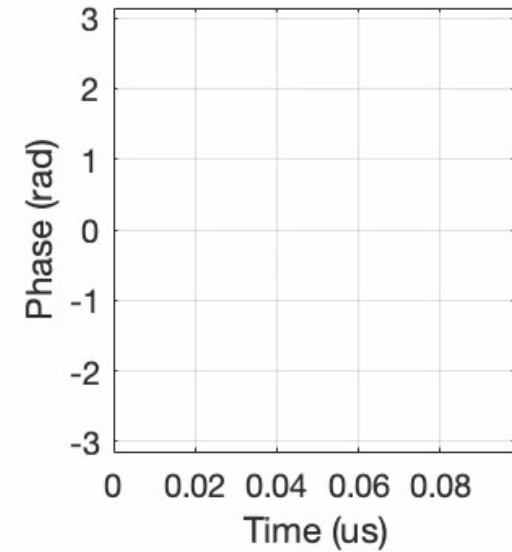
Precession of Magnetization



Magnitude

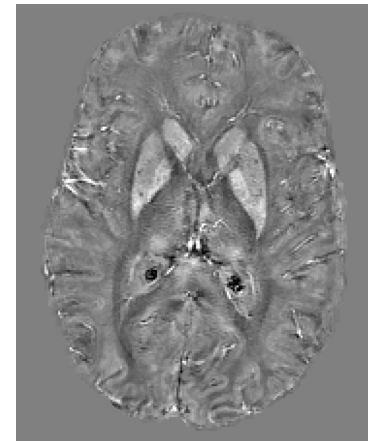
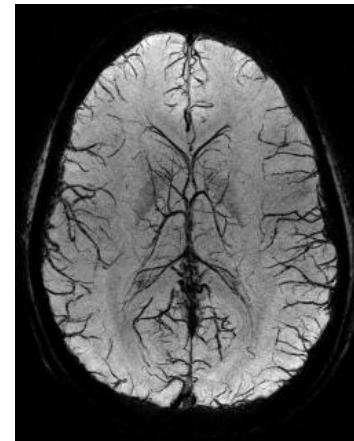
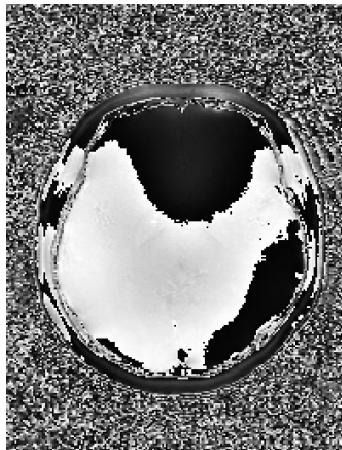
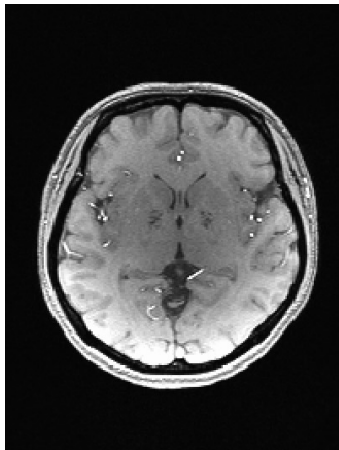
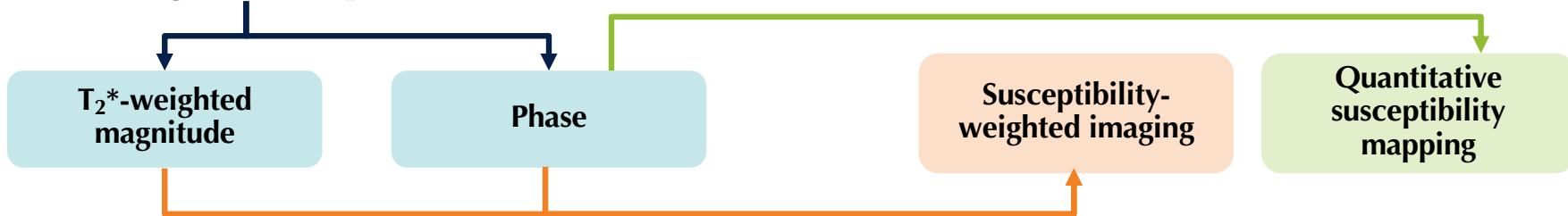


Phase



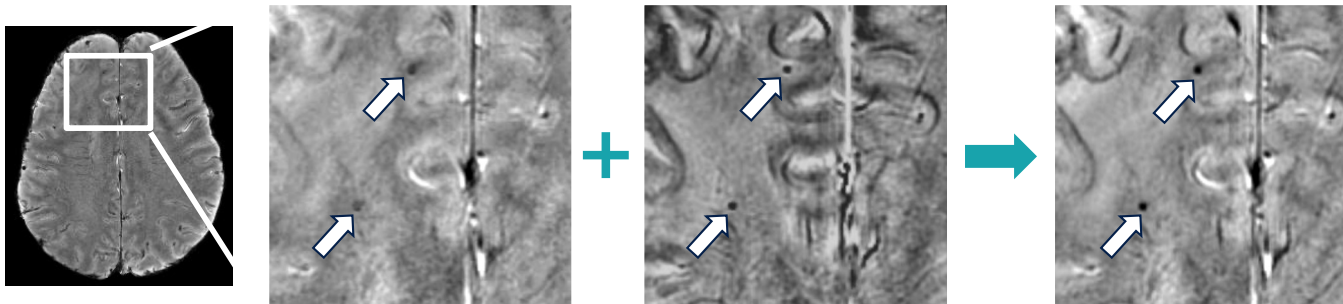
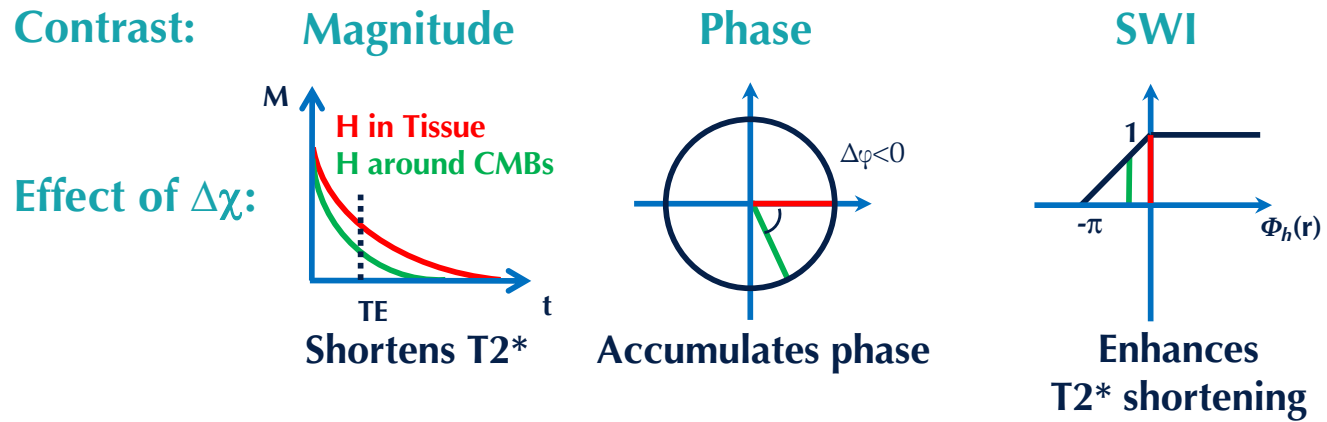
# Susceptibility MRI – Signal model

$T_2^*$ -weighted sequence

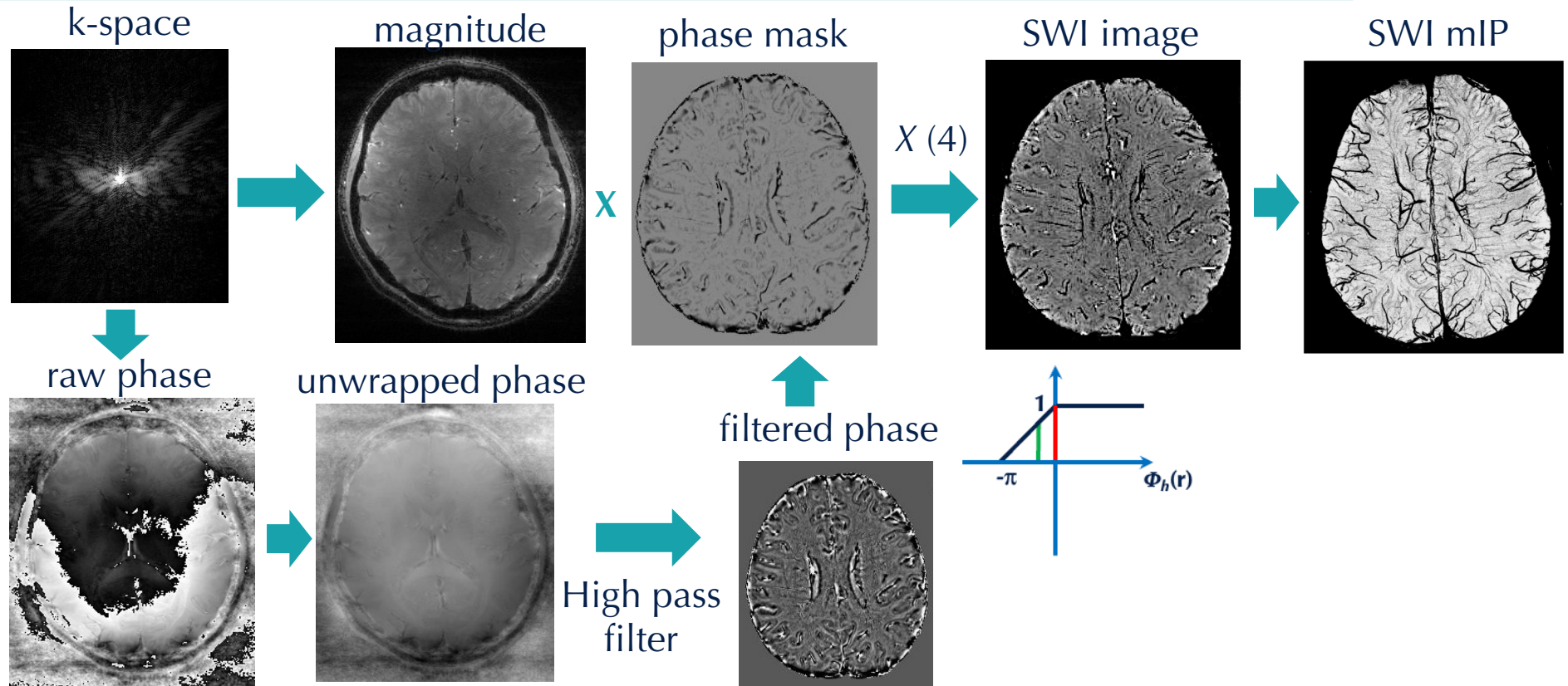




# Susceptibility MRI – Signal model

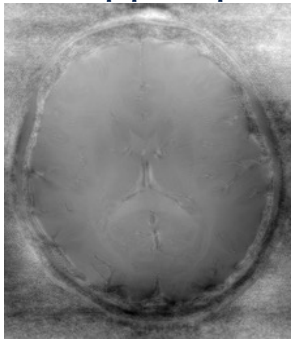


# SWI – Processing

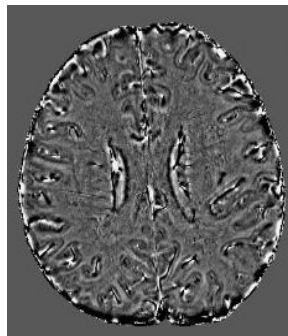


# SWI – Processing

unwrapped phase

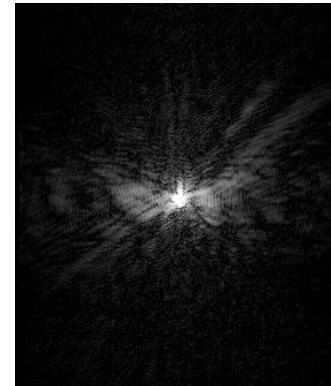


filtered phase

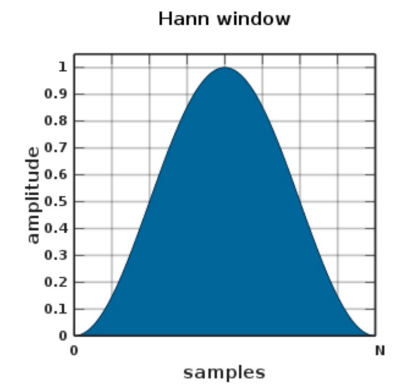


High pass  
filter

Complex division

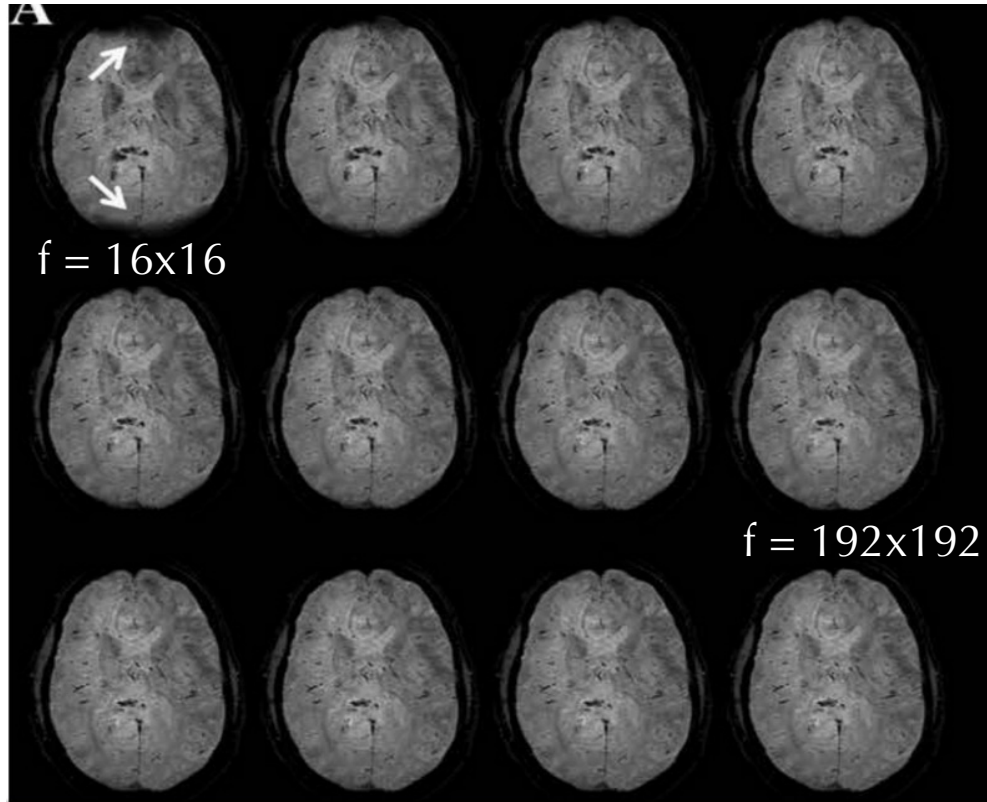
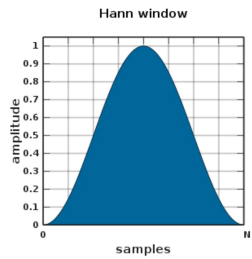


X



Low pass filtered  
phase

# SWI – Processing



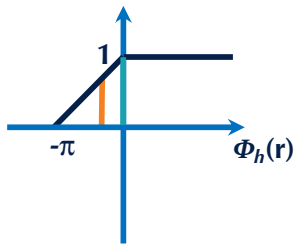
Higher contrast,  
more artifacts



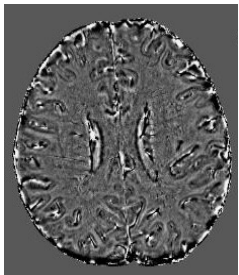
lower contrast,  
less artifacts

# SWI – Processing

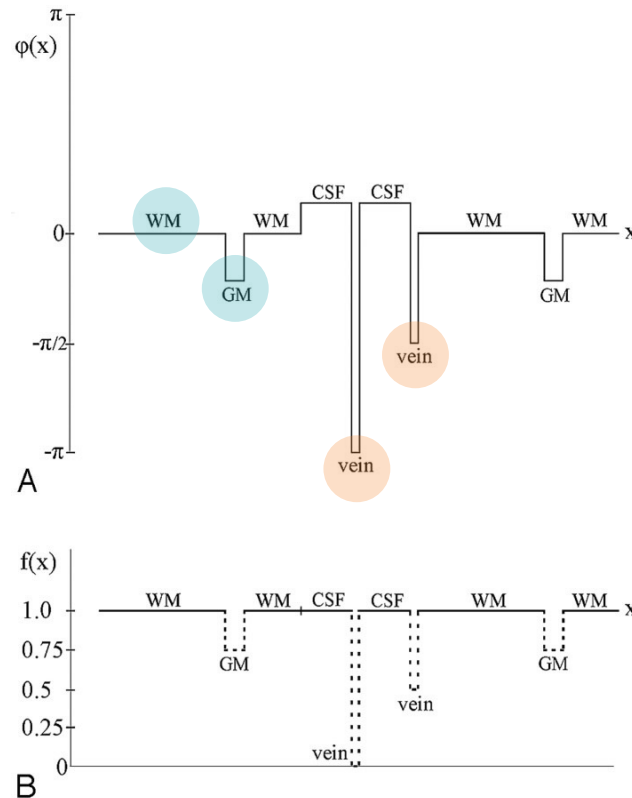
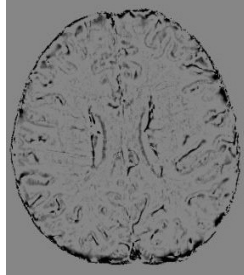
## SWI phase masking



filtered phase



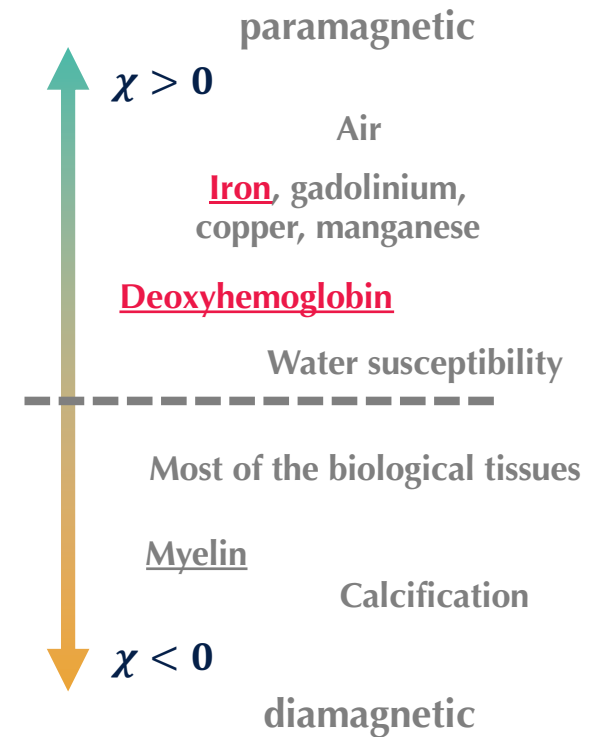
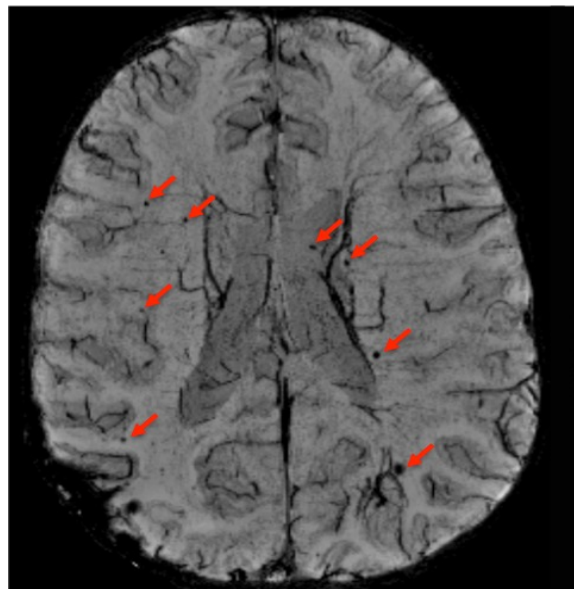
phase mask



	WM	GM	Vein (small)	Vein (Large)
Phase	0	$-0.25\pi$	$-0.5\pi$	$-\pi$
$f(x)^1$	1	0.75	0.5	0
$f(x)^2$	1	0.56	0.25	0
$f(x)^3$	1	0.42	0.13	0
$f(x)^4$	1	0.32	0.06	0

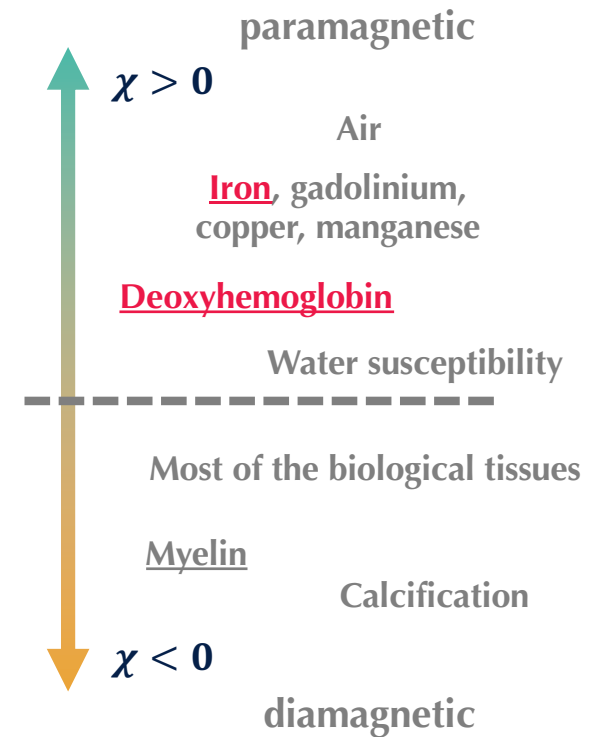
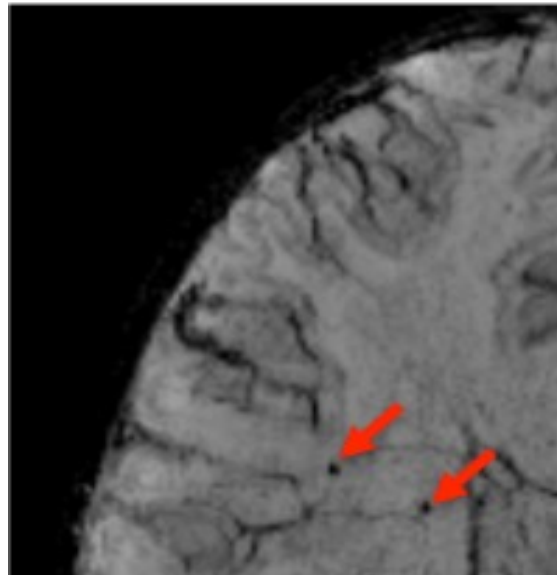
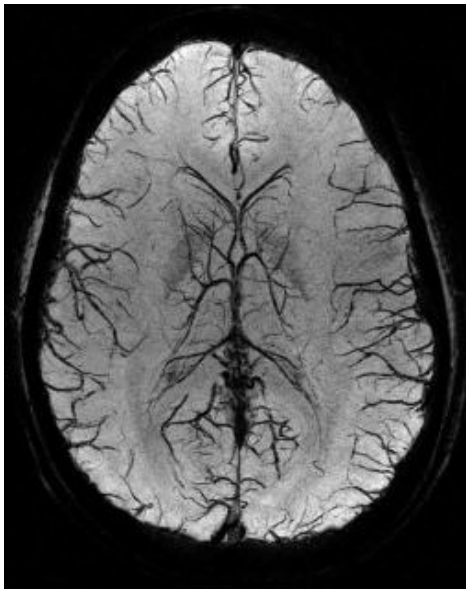
# SWI – Example applications

phase-weighted magnitude imaging



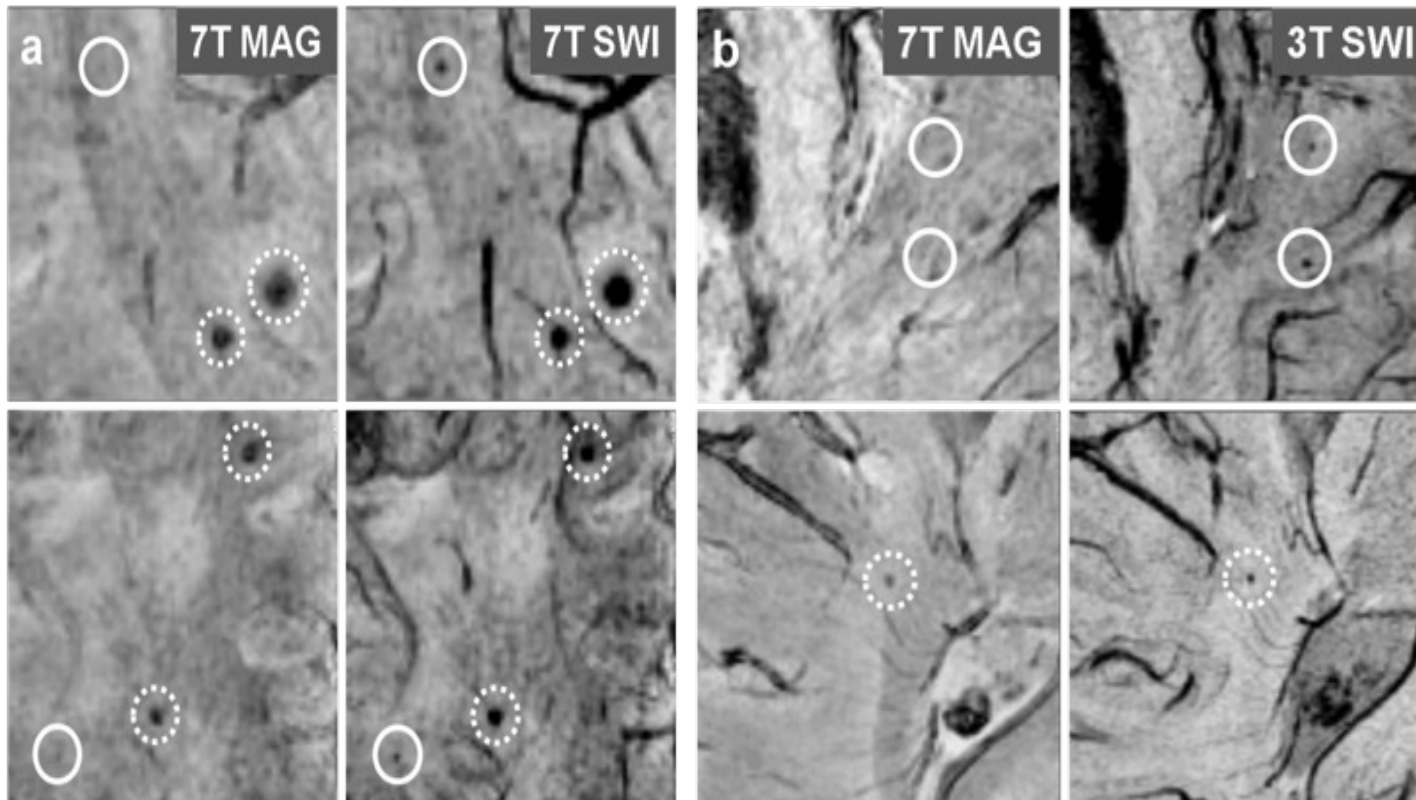
# SWI – Example applications

phase-weighted magnitude imaging



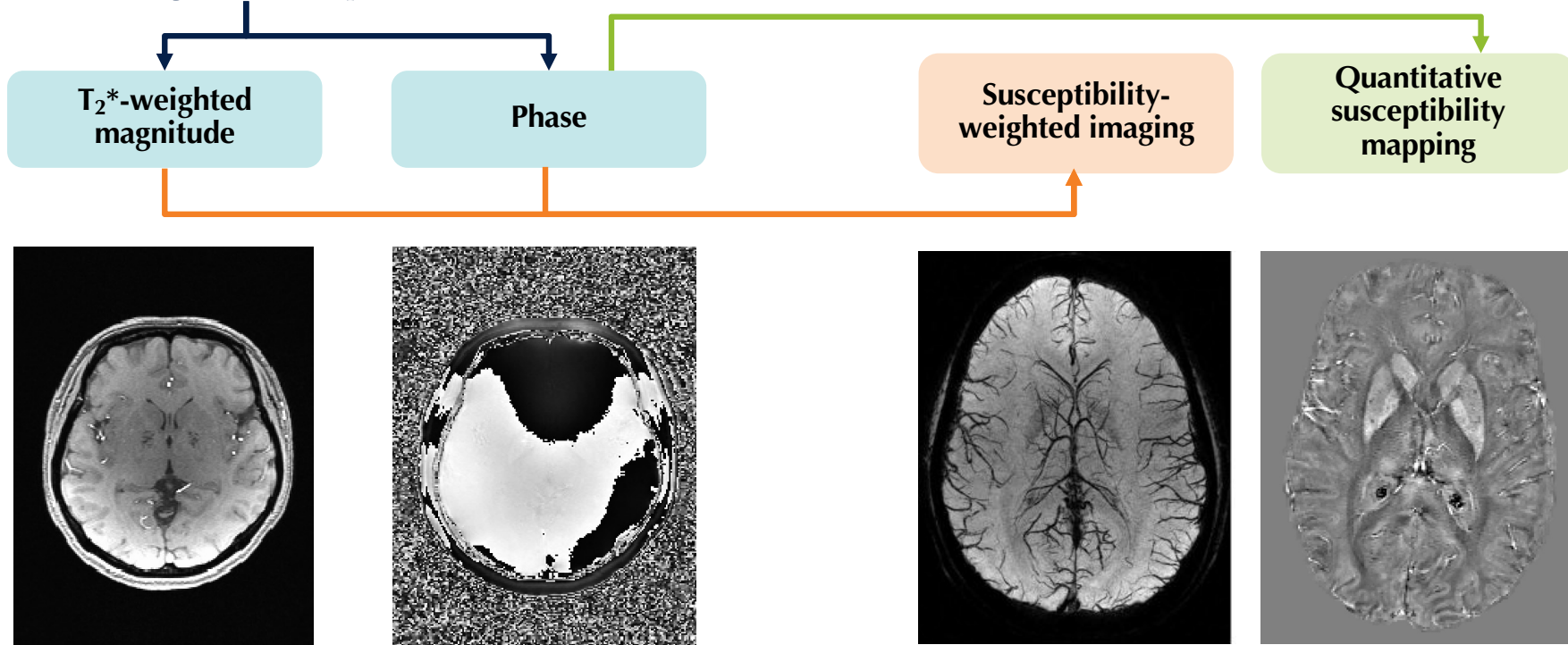


## SWI – Example applications

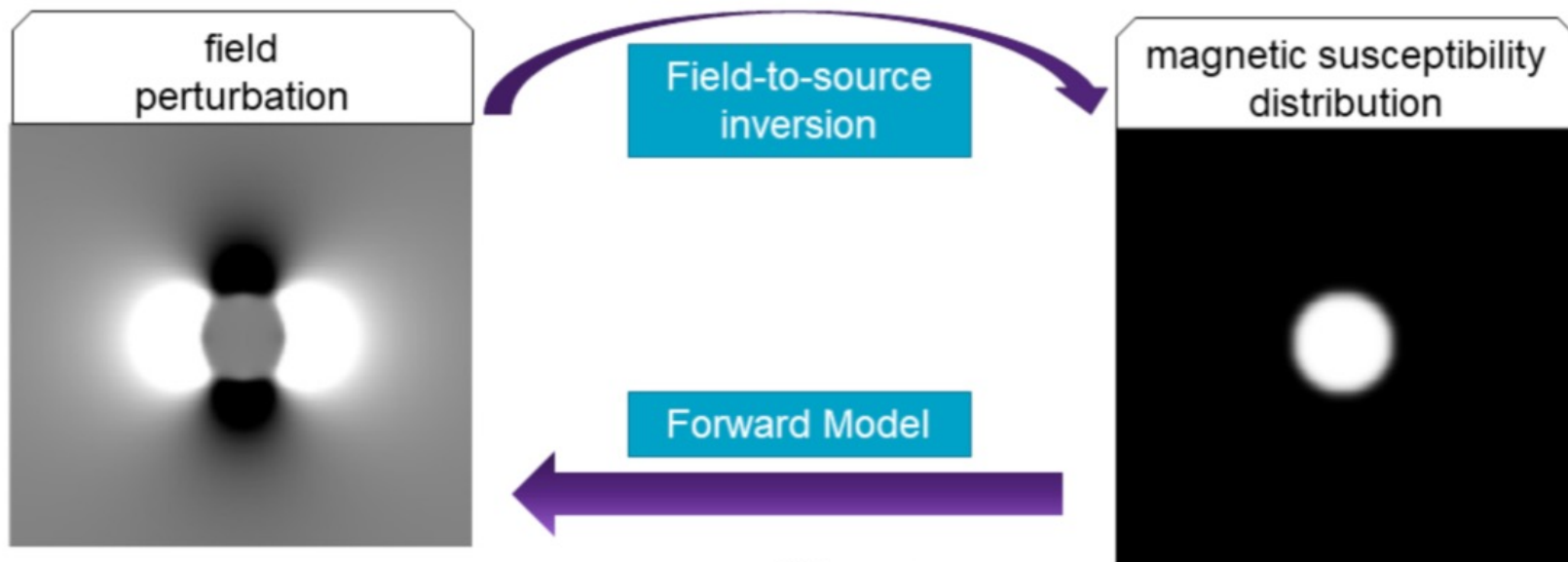


# Susceptibility MRI – source of contrast

## $T_2^*$ -weighted sequence



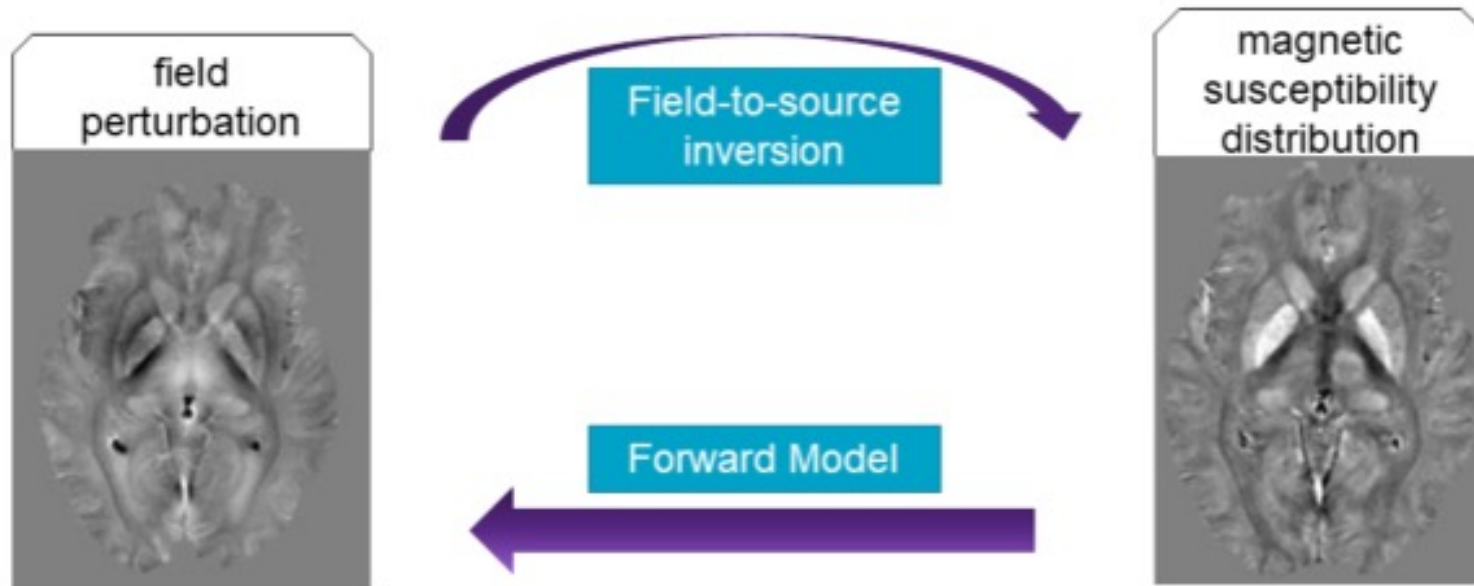
## Susceptibility MRI – Signal model



$$\Delta B_{\text{int}}(\vec{r}) = B_0 \cdot \int_{-\infty}^{\infty} \tilde{\chi}(\vec{r}') \cdot d_z(\vec{r} - \vec{r}') d^3 \vec{r}'$$

Review: Deistung et al. NMR Biomed 2017; Schweser et al. Z Med Phys 2016

# Susceptibility MRI – Signal model



$$\Delta B_{\text{int}}(\vec{r}) = B_0 \cdot \int_{-\infty}^{\infty} \tilde{\chi}(\vec{r}') \cdot d_z(\vec{r} - \vec{r}') d^3 \vec{r}'$$

What is it called?

Review: Deistung et al. NMR Biomed 2017; Schweser et al. Z Med Phys 2016



# Susceptibility MRI – Signal model

$$\Delta B(\vec{r}) = B_0 \int_{-\infty}^{\infty} \chi(\vec{r}') d(\vec{r} - \vec{r}') d^3 \vec{r}'$$

$$d(\vec{r}) = \frac{1}{4\pi} \frac{3 \cos^2(\theta) - 1}{|\vec{r}|^3}$$

$$\Delta B = B_0(\chi \otimes d)$$

Known

Measured

Unknown



What is the FT of convolution?

FT

$$\Delta B(\vec{k}) = B_0[\chi(\vec{k})d(\vec{k})]$$

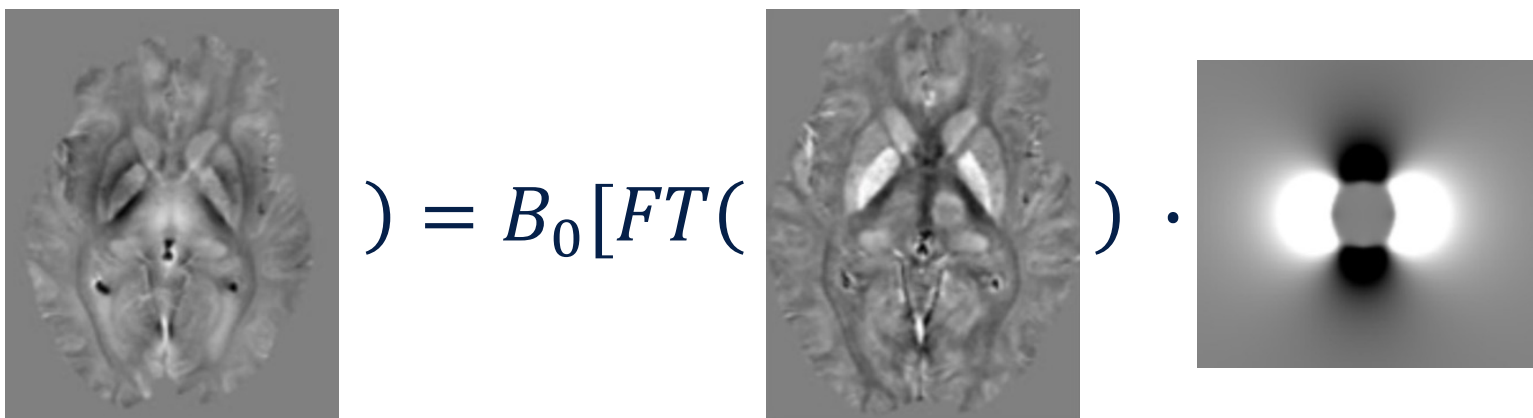
$$d(\vec{k}) = \frac{1}{3} - \frac{k_z^2}{|\vec{k}|^2}$$



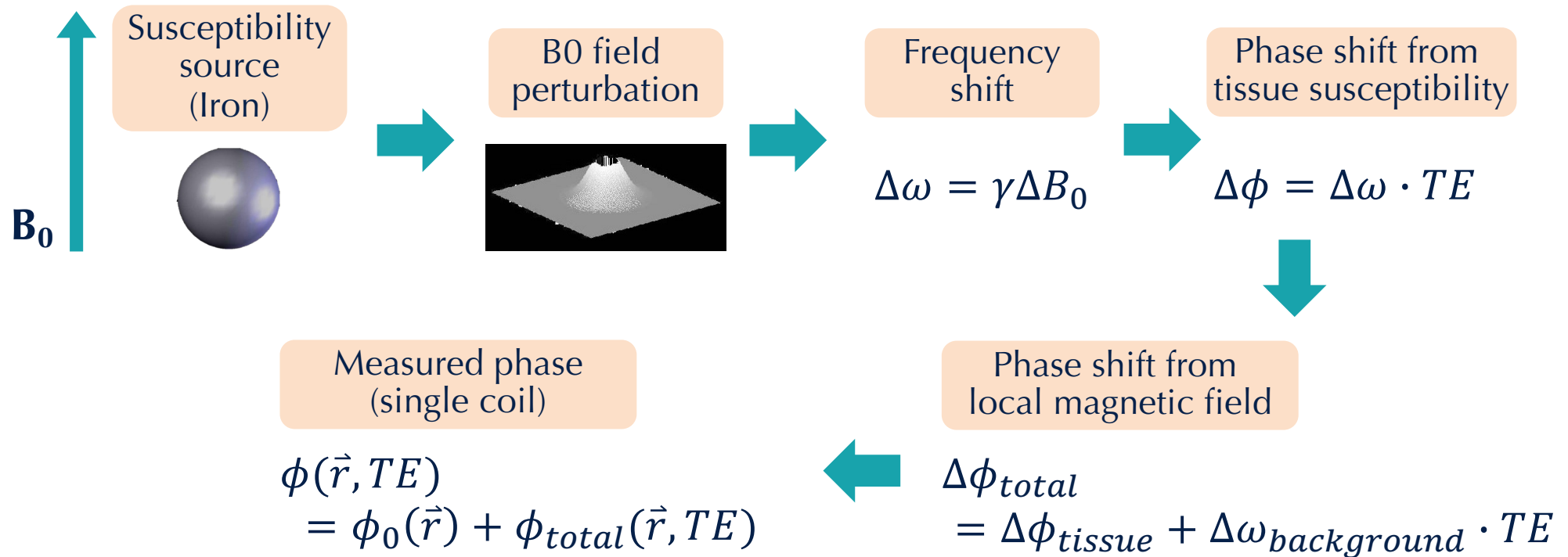
## Susceptibility MRI – Signal model

$$\Delta B(\vec{k}) = B_0[\chi(\vec{k})d(\vec{k})]$$

$$d(\vec{k}) = \frac{1}{3} - \frac{k_z^2}{|\vec{k}|^2}$$

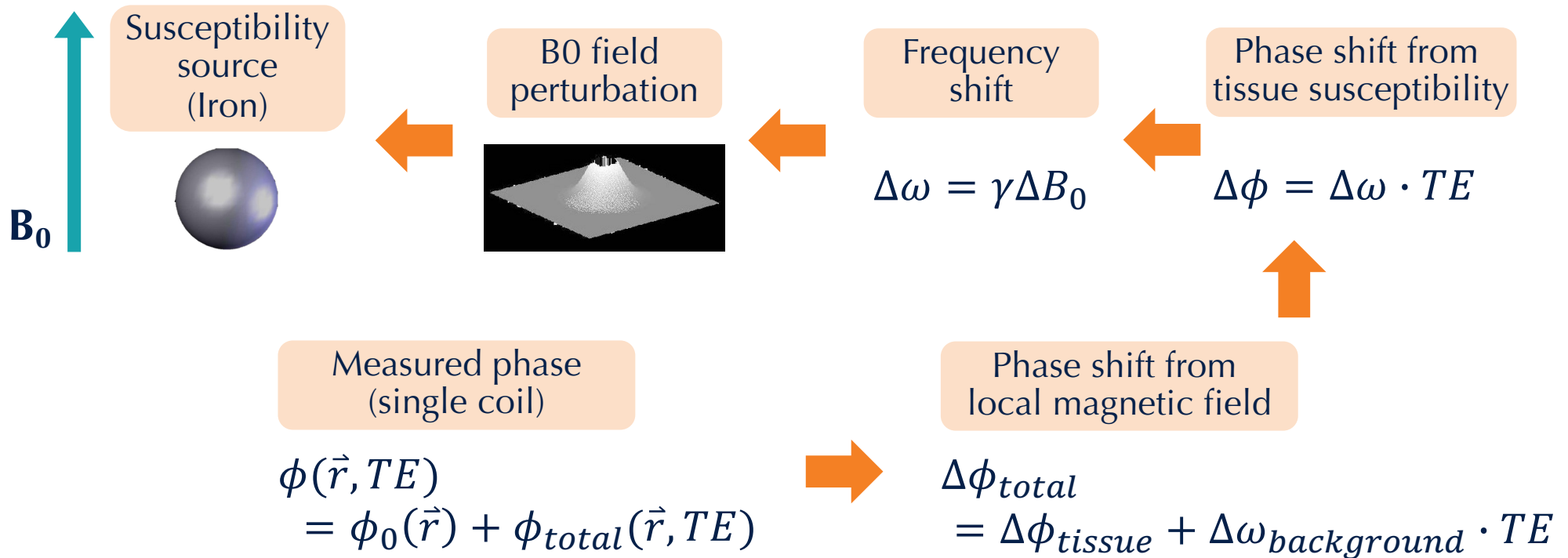
$$FT(\text{Image 1}) = B_0[FT(\text{Image 2}) \cdot \text{Image 3}]$$


# Susceptibility MRI – Signal model





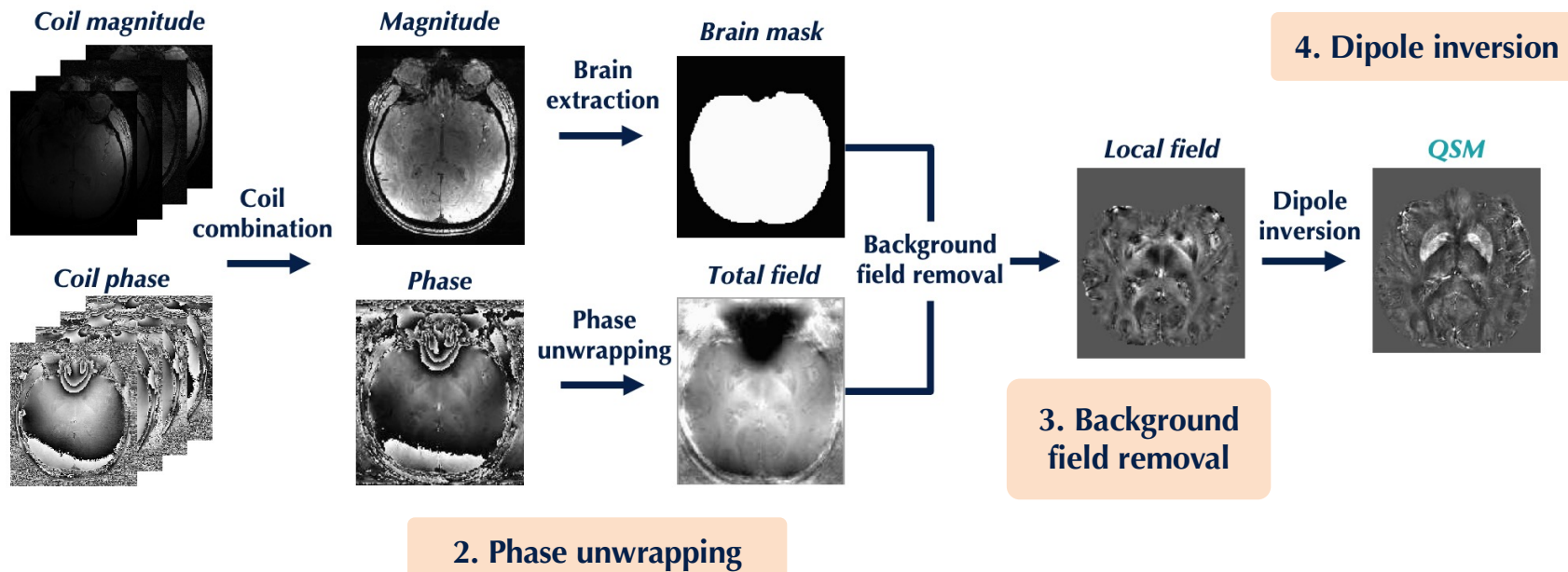
# Susceptibility MRI – Processing



# QSM - Processing

## 1. Coil combination

$T_2^*$ -weighted sequence



# QSM - Processing

## 1. Coil combination

$T_2^*$ -weighted sequence

*Coil magnitude*

Phase combination approaches

1 echo,  
No reference scan

- Scalar phase matching [1]
- Adaptive combine [2]
- Virtual Reference Coil [3]

1 echo,  
Reference scan

- Roemer/SENSE [4]
- COMPOSER [5]

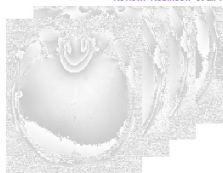
Multiple echoes

- SVD [6]
- Solve for  $\Delta B_0$  via phase difference [7]
- Solve for  $\phi_0^i$ : ASPIRE [8]

[1] Hammond et al. NI 2008  
[2] Walsh et al. MRM 2000  
[3] Parker et al. MRM 2014

[4] Roemer et al. NI 1990  
[5] Robinson et al. MRM 2017  
Review: Robinson et al. NMR Biomed 2017

[6] Khabipova et al. NI 2015  
[7] Bernstein et al. MRM 1994  
[8] Dickert et al. MRM 2018



*Magnitude*

Unwrapping techniques

Laplacian

- differentiable operator applied to the unwrapped phase can produce the same result on the wrapped phase  $\rightarrow$  Laplacian (Schofield and Zhu, Opt. Lett. 2003)
- + fast & robust
- - introduces background phase

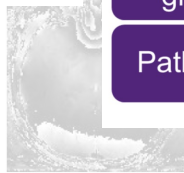
Region-growing

- identify discontinuities between regions
- PRELUDE (Jenkinson MRM 2003) can take a while to compute for highly wrapped data
- SEGUE (Karsa et al. TMI 2019) similar accuracy to PRELUDE, but faster

Path Based

- 3D voxel-by-voxel unwrapping guided by the quality of voxel connections
- BEST PATH (Abdul-Rahman et al. AO 2007)
- ROMEO (Dymerska et al. MRM 2021)

Review: Robinson et al., NMR Biomed 2017



## 2. Phase unwrapping

Background field correction methods & assumptions

no sources close to boundaries

- SHARP (Schweser et al. NI 2011)
- V-SHARP (Li et al. NI 2011)

no harmonic internal and boundary fields

- LBV (Zhou et al. NMR Biomed 2014)

no implicit boundary assumption

- RESHARP (Sun et al. MRM 2014)
- SHARQnet (Bollmann et al. Z Med Phys 2018)

Review: Schweser et al. NMR Biomed 2017

*Local*



## 3. Background field removal

## 4. Dipole inversion

Dipole inversion methods & assumptions

multiple orientations

- COSMOS (Liu et al. MRM 2009)
- STI (Liu MRM 2010)
- analytical solutions, but not practical

inverse filtering

- TKD (Shmueli et al. MRM 2009)
- fast, but need parameter tweaking

iterative methods

- LSQR (Li et al. NI 2015)
- MEDI (Liu et al. MRM 2013)
- slow, need parameter tweaking

agnostic deep learning

- QSMnet (Yoon et al. NI 2018)
- DeepQSM (Bollmann et al. NI 2019)
- fast, but fragile

hybrid methods

- FINE (Zhang et al. NI 2020)
- Variational Networks (Liu et al. arXiv 2020)
- Deep learning priors + data consistency constraints

Reviews: Schweser et al. NMR Biomed 2017; Jung et al. NMR Biomed 2020

# QSM - Coil Combination

**NMR**  
IN BIOMEDICINE

## Special issue review article

Received: 11 November 2015,

Revised: 14 June 2016,

Accepted: 18 July 2016,

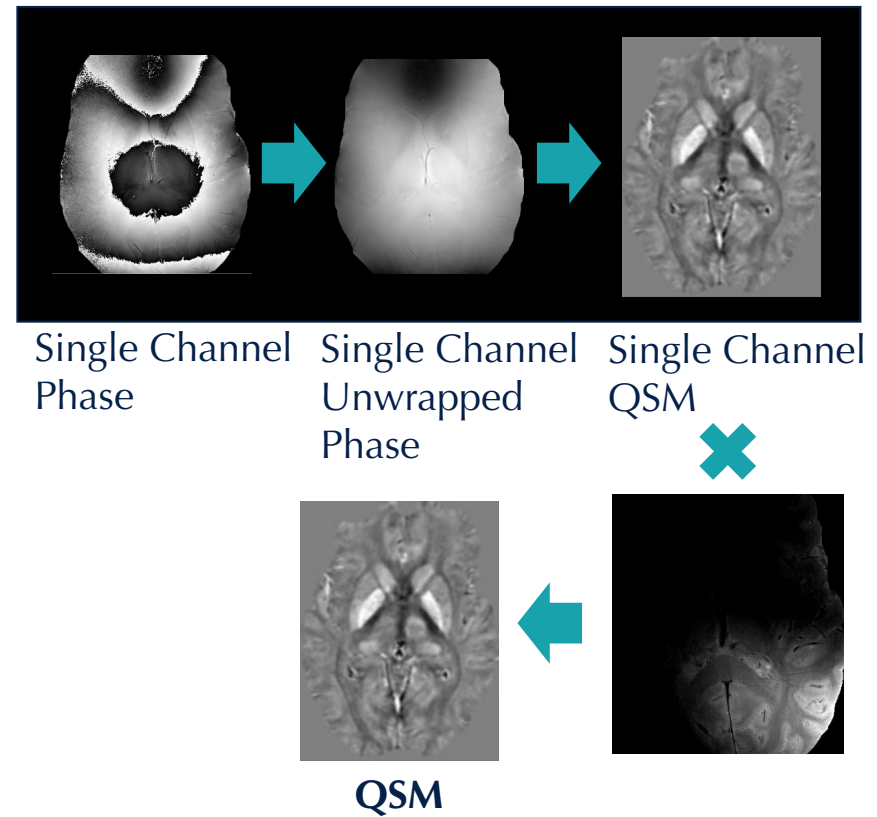
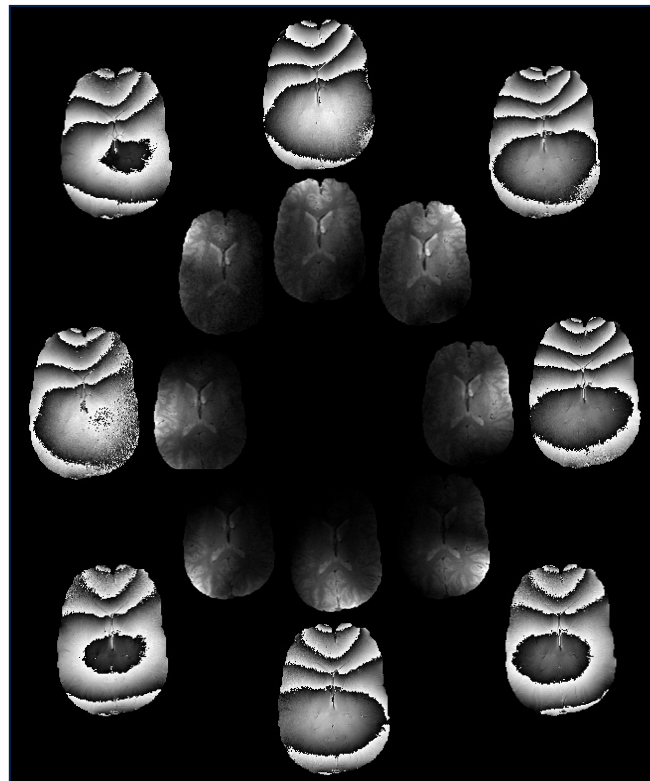
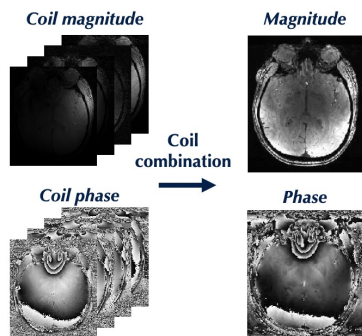
Published online in Wiley Online Library: 13 September 2016

(wileyonlinelibrary.com) DOI: 10.1002/nbm.3601

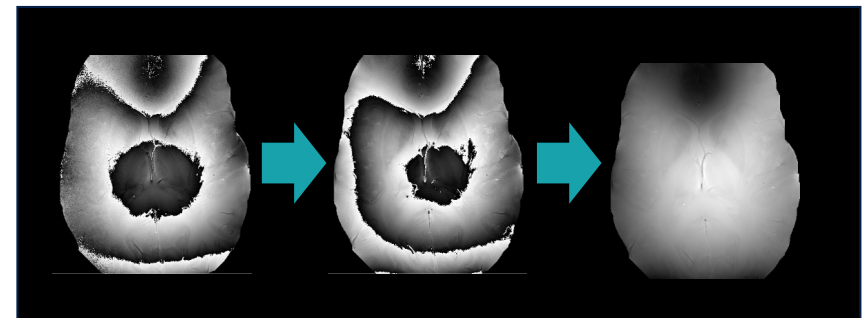
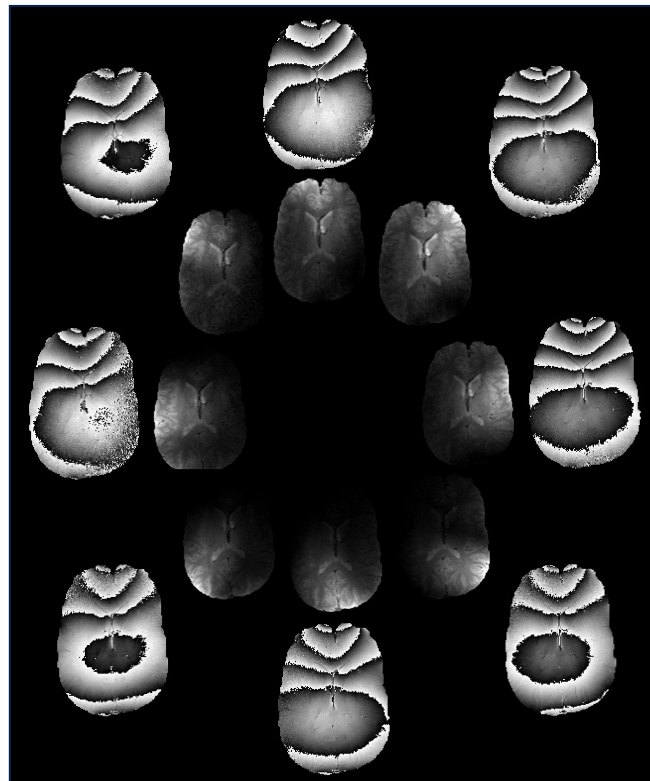
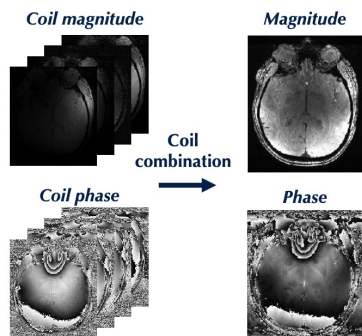
## **An illustrated comparison of processing methods for MR phase imaging and QSM: combining array coil signals and phase unwrapping**

**Simon Daniel Robinson<sup>a\*</sup>, Kristian Bredies<sup>b</sup>, Diana Khabipova<sup>c,d</sup>,  
Barbara Dymerska<sup>a</sup>, José P. Marques<sup>c,d</sup> and Ferdinand Schweser<sup>e,f</sup>**

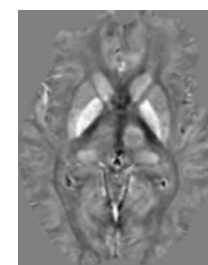
# QSM - Coil Combination



# QSM - Coil Combination



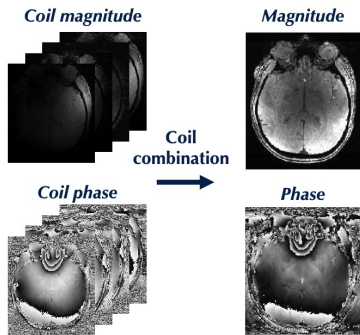
Single Channel Phase    Multi Channel Phase    Unwrapped Phase



QSM



# QSM - Coil Combination

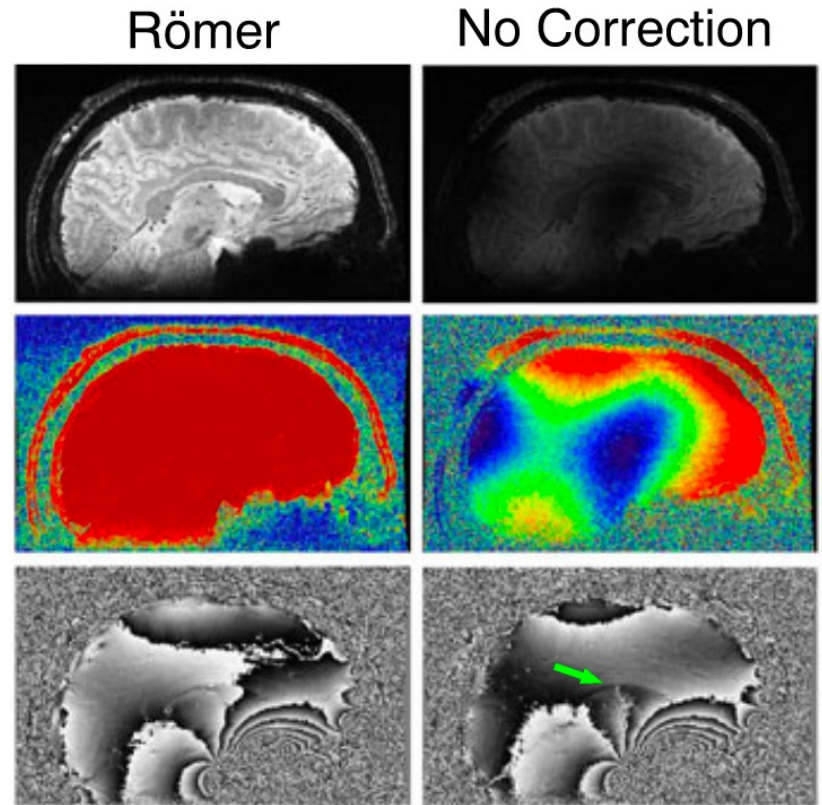


Measured phase  
(single coil)

$$\phi(\vec{r}, TE) = \phi_0(\vec{r}) + \phi_{total}(\vec{r}, TE)$$

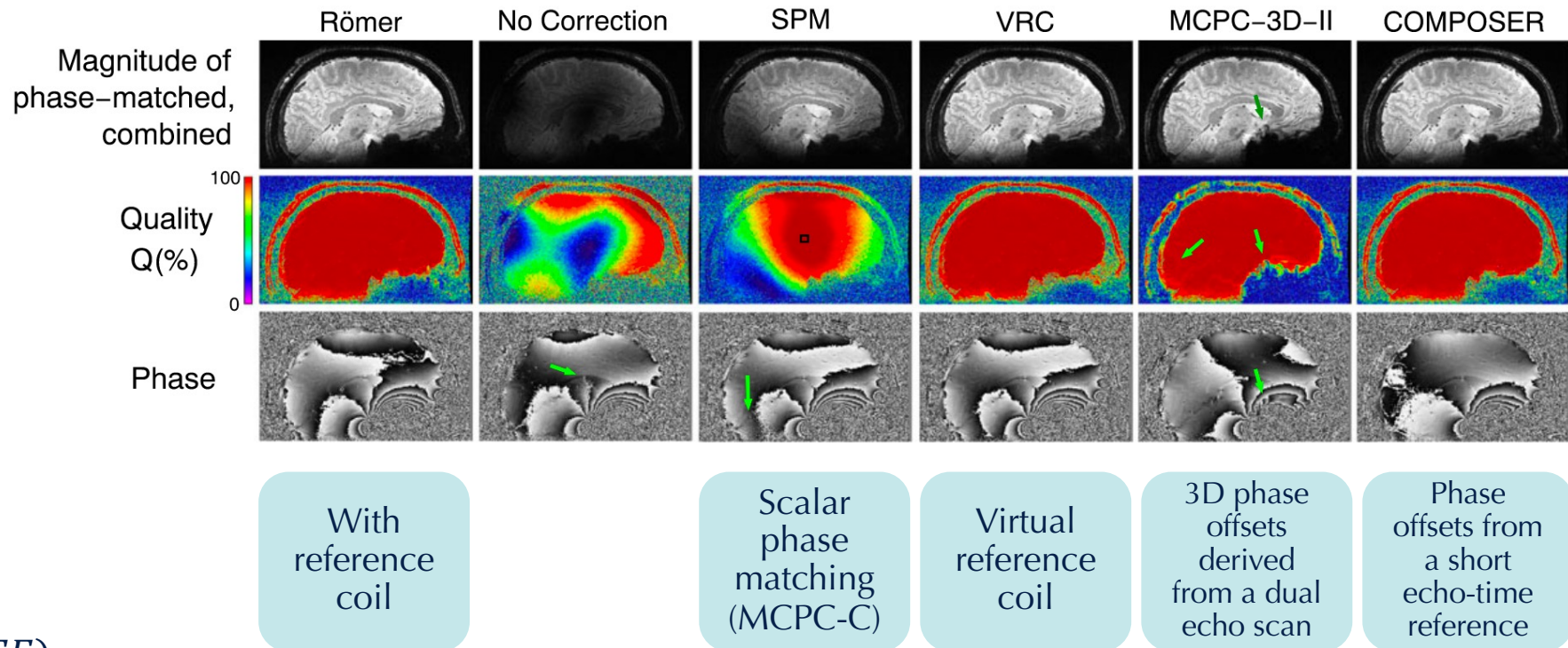
Transceiver phase

spatially varying phase  
offsets exist between  
receive coils





# QSM - Coil Combination



$$\phi(\vec{r}, TE) = \phi_0(\vec{r}) + \phi_{total}(\vec{r}, TE)$$

$$\phi_j^0(\vec{r}) = \frac{\phi_j(\vec{r}, TE_2)TE_1 - \phi_j(\vec{r}, TE_1)TE_2}{TE_1 - TE_2}$$

## QSM – MCPC-3D

### Steps:

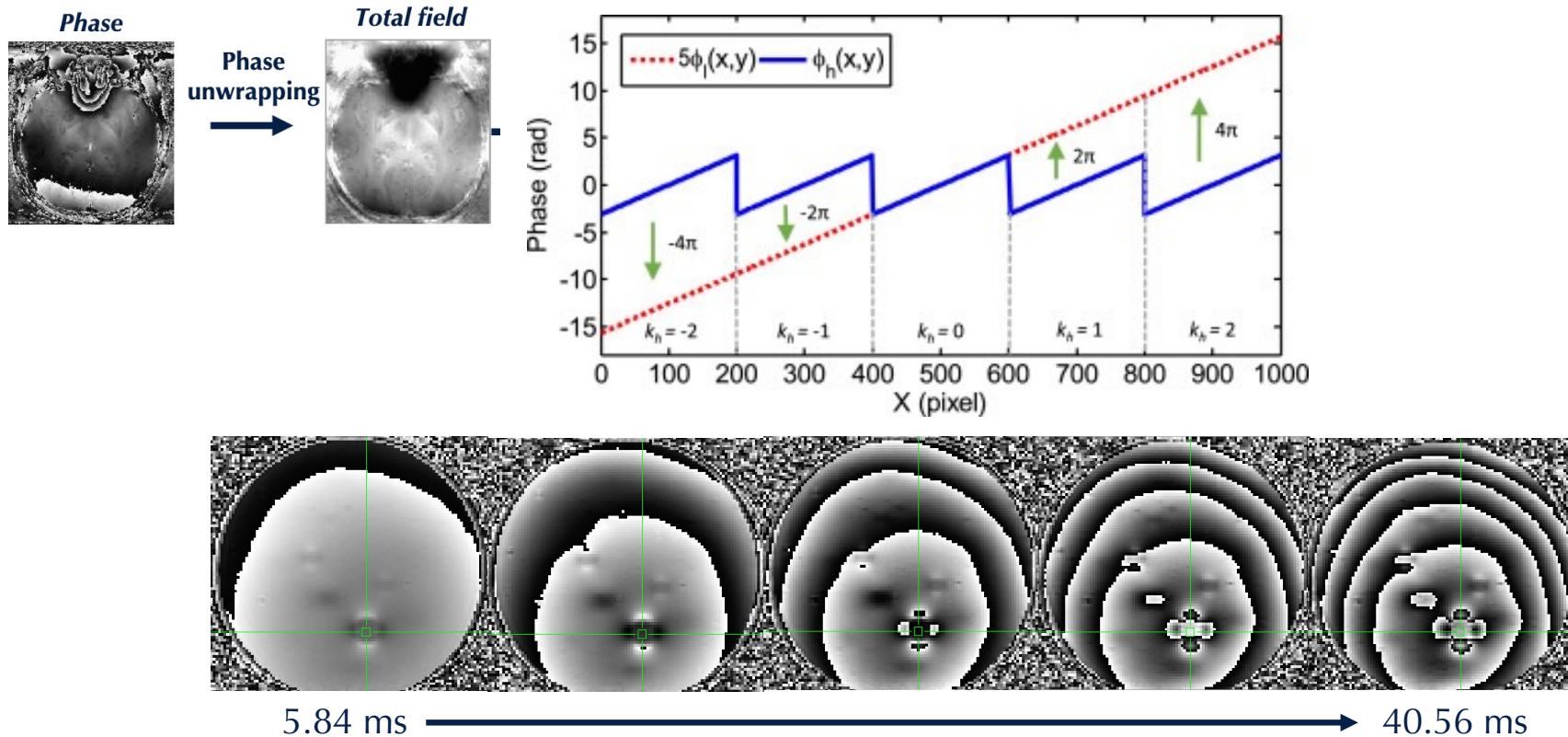
- unwrap each echo phase
- create 3D phase offset map for each coil using each unwrapped echo
- smooth with 5x5 median filter (complex smoothing)
- subtract 3D phase offset map from phase image of each channel
- weighted mean

$$\phi_j^0(\vec{r}) = \frac{\phi_j(\vec{r}, TE_2)TE_1 - \phi_j(\vec{r}, TE_1)TE_2}{TE_1 - TE_2}.$$

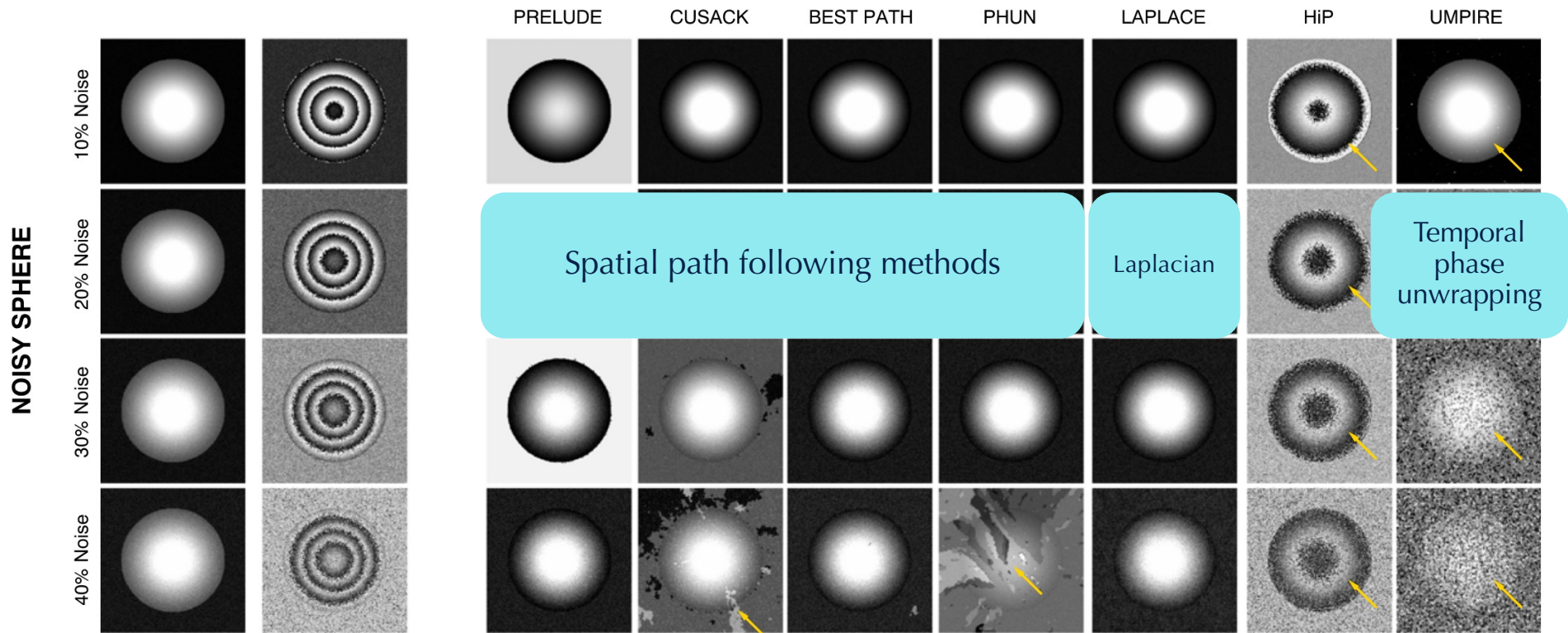
### Advantages:

- works where there is no signal overlap between receivers
- no need for reference coil
- also works using a separate low-resolution scan

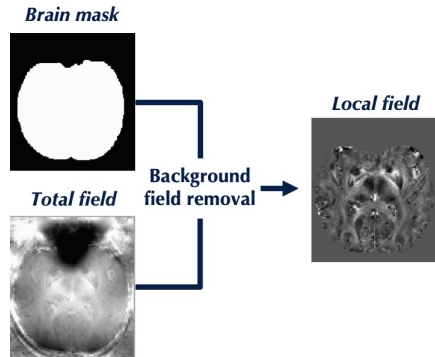
# QSM - Phase unwrapping



# QSM - Phase unwrapping



# QSM - Background field removal



Journal of Magnetic Resonance 148, 442–448 (2001)  
doi:10.1006/jmre.2000.2267, available online at <http://www.idealibrary.com> on IDEAL®

## High-Precision Mapping of the Magnetic Field Utilizing the Harmonic Function Mean Value Property

Lin Li and John S. Leigh

Department of Biochemistry and Molecular Biophysics, and Metabolic Magnetic Resonance Research & Computing Center, Department of Radiology, University of Pennsylvania, Philadelphia, Pennsylvania 19104

Received June 15, 2000; revised November 20, 2000

The spatial distributions of the static magnetic field components and MR phase maps in space with homogeneous magnetic susceptibility are shown to be harmonic functions satisfying Laplace's equation. A mean value property is derived and experimentally confirmed on phase maps: the mean value on a spherical surface in space is equal to the value at the center of the sphere. Based on this property, a method is implemented for significantly improving the precision of MR phase or field mapping. Three-dimensional mappings of the static magnetic field with a precision of  $10^{-11} \sim 10^{-12}$  T are obtained in phantoms by a 1.5-T clinical MR scanner, with about three-orders-of-magnitude precision improvement over the conventional phase mapping technique. *In vivo* application of the method is also demonstrated on human leg phase maps. © 2001

Academic Press

**Key Words:** field mapping; harmonic function; mean value property; phase; SMV.

aging, we generate field maps with high precision up to  $10^{-11} \sim 10^{-12}$  T. Such a measurement precision is comparable with that of a superconducting quantum interference device (SQUID) for the magnetic field measurement (17). Feasibility with *in vivo* applications is also demonstrated.

### THEORY

In free space or regions without susceptibility heterogeneity and no macroscopic currents, all the components of the static magnetic field  $\mathbf{H}$  satisfy Laplace's equation, i.e.,  $\nabla^2 \mathbf{H}_i = 0$ ,  $i = x, y, z$ , or  $\nabla^2 \mathbf{H} = 0$ , which can be easily derived by setting the temporal derivative of the magnetic field in the electromagnetic wave equation (18) to zero. Therefore, local magnetic induction (4, 19) experienced by a nucleus,  $(1 + \chi/3)H$ , also satisfies Laplace's equation. Since the spatial

VSHARP

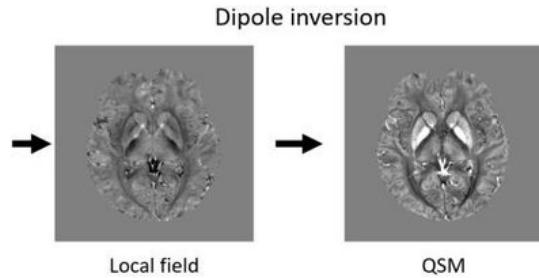
RESHARP

HARPERELLA

PDF

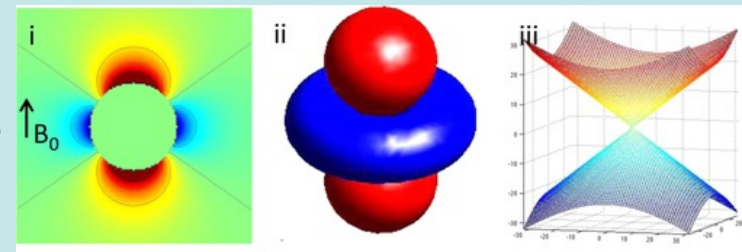


# QSM - Dipole Inversion



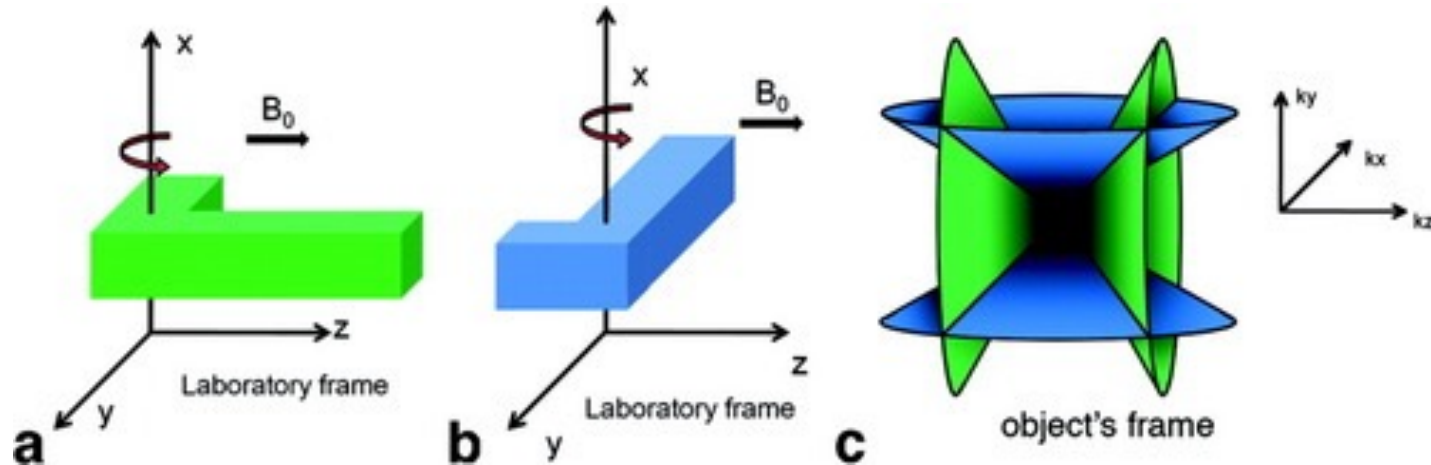
$$FT(\text{Local field}) = B_0 [FT(\text{QSM}) \cdot \text{Dipole kernel}]$$

**ill-posed inversion problem**  
Noise amplification near the  
zero cone surfaces



# QSM - Dipole Inversion

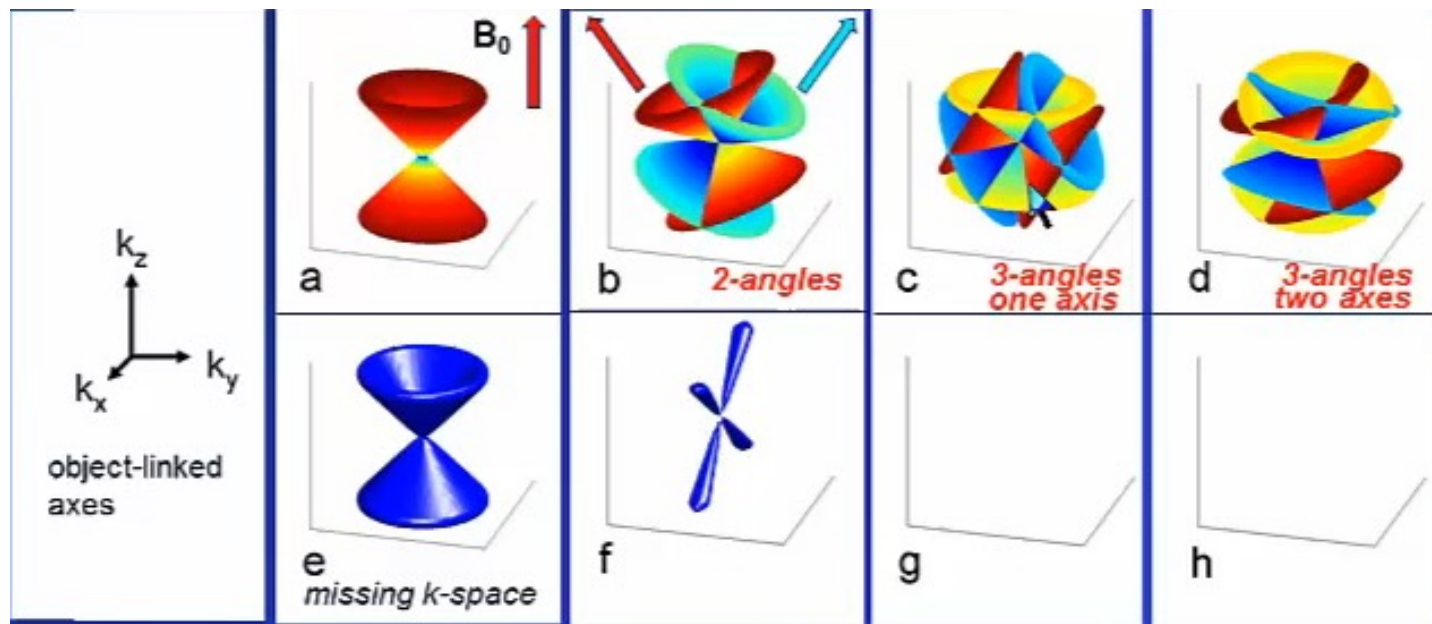
**COSMOS:** calculation of susceptibility using multiple orientation sampling





# QSM - Dipole Inversion

**COSMOS:** calculation of susceptibility using multiple orientation sampling

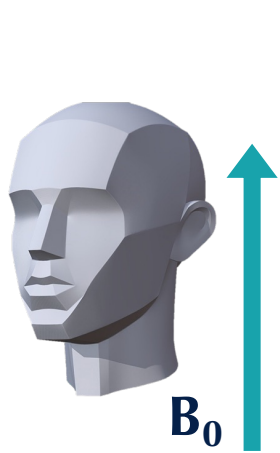


# QSM - Dipole Inversion

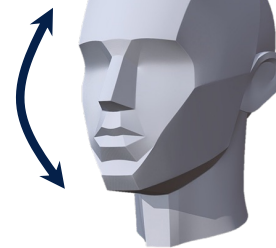
**COSMOS:** calculation of susceptibility using multiple orientation sampling



How would you reorient?



A. Rotation along z



B. Up/down  
nodding

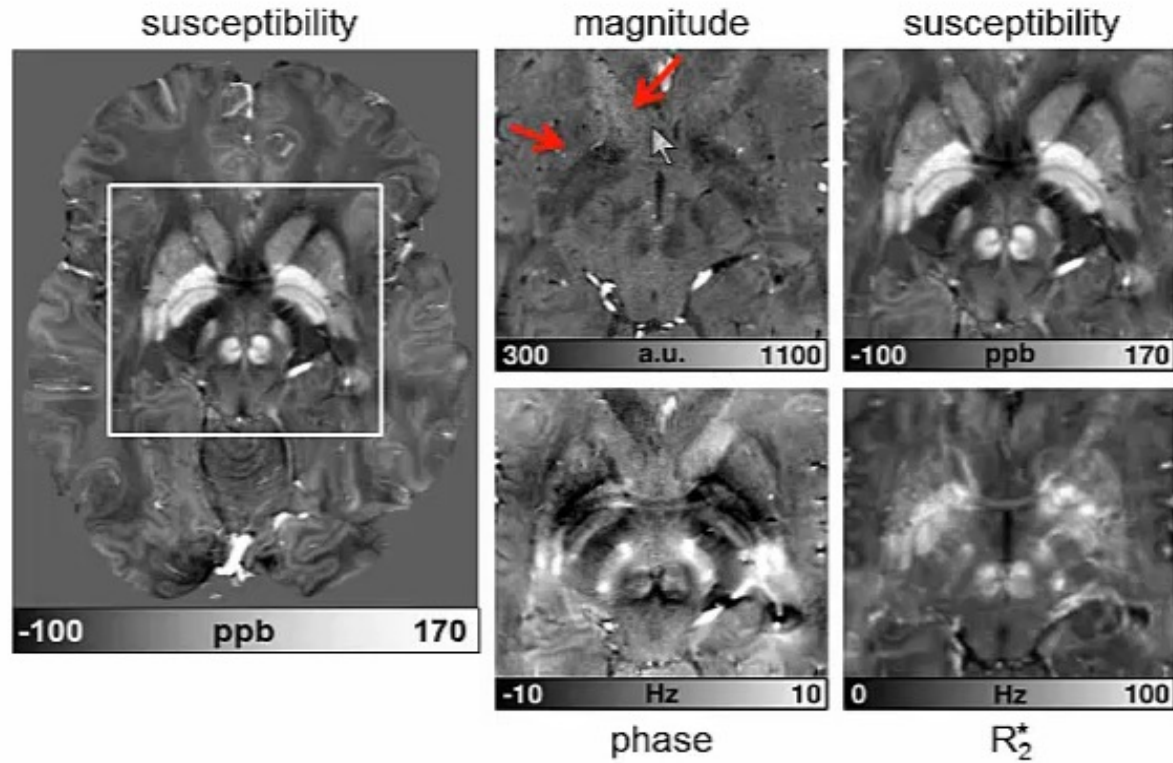


C. Right/left  
head tilt



# QSM - Dipole Inversion

COSMOS:



Deistung, A et al. NeuroImage 2013, 65, 299–314.

# QSM Dipole Inversion: TKD

**TKD:** Truncated K-space Division

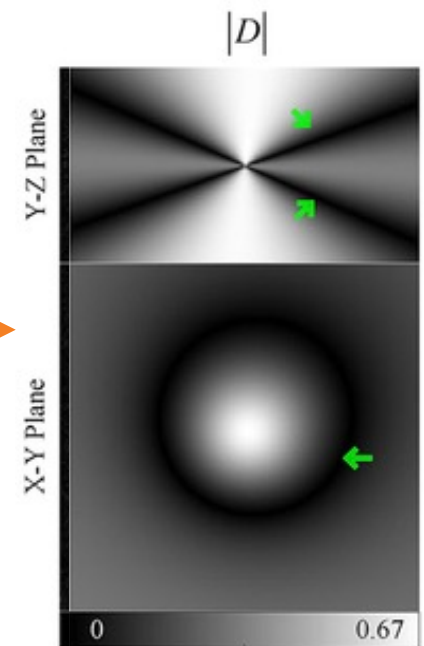
Dipole kernel

$$\psi(\mathbf{k}) = D_2(\mathbf{k}) \cdot \chi(\mathbf{k})$$

Field perturbation

Susceptibility distribution

$$\rightarrow D_2(k) = \begin{cases} D_2(k) & \text{if } |D_2(k)| \geq \delta \\ \delta \cdot \text{sign}(D_2(k)) & \text{otherwise} \end{cases}$$



# QSM Dipole Inversion: iLSQR

**iLSQR:** iterative method solving least square using the orthogonal and right triangular decomposition

Dipole kernel

$$\psi(\mathbf{k}) = D_2(\mathbf{k}) \cdot \chi(\mathbf{k})$$

Field perturbation

Susceptibility distribution

1<sup>st</sup> order derivative

$$\psi'(\mathbf{k}) + [2(k_x^2 + k_y^2)k_z/k^4] \cdot \chi(\mathbf{k}) - D_2(\mathbf{k}) \cdot \chi'(\mathbf{k}) = 0$$

$$D_3(\mathbf{k}) \cdot \chi(\mathbf{k}) + D_2(\mathbf{k}) \cdot FT[i \cdot r_z \chi(\mathbf{r})] = FT[i \cdot r_z \psi(\mathbf{r})]$$

$$\chi(\mathbf{k}) = D_2(\mathbf{k})^{-1} \cdot \psi(\mathbf{k}), \text{ when } D_2(\mathbf{k}) \geq \varepsilon$$

$$\chi(\mathbf{k}) \approx D_3(\mathbf{k})^{-1} \cdot FT[ir_z \psi(\mathbf{r})], \text{ when } D_2(\mathbf{k}) < \varepsilon$$

Where:  $D_3(\mathbf{k}) = (k_x^2 + k_y^2)k_z/\pi k^4$

## QSM Dipole Inversion: iterative inversion methods with regularization

Recon problem

$$\operatorname{argmin}_{\chi} \frac{1}{2} \left\| W(F^H D F \chi - \Phi) \right\|_2^2 + \alpha \Omega(\chi)$$

Data consistency term

Regularization term

Nonlinear variant

$$\operatorname{argmin}_{\chi} \frac{1}{2} \left\| W \left( e^{i F^H D F \chi} - e^{i \Phi} \right) \right\|_2^2 + \alpha \Omega(\chi)$$

Method	Data consistency term	Regularization term
STAR-QSM (STreaking Artifact Reduction for QSM)	Linear L2-norm	Total variation
FANSI (FAst Nonlinear Susceptibility Inversion)	Nonlinear L2-norm	Total variation
HD-QSM (Hybrid Data fidelity)	Linear L1+L2-norm	Total variation
MEDI (Morphology Enabled Dipole Inversion)	Linear L1-norm	L1 norm of morphologically weighted gradients

## QSM Dipole Inversion: single step methods

### QSIP

Quantifying Susceptibility by Inversion of a Perturbation model

$$\chi_1^* = \arg \min_{\chi_1} \left[ \lambda_1 \|W \circ (\Delta B - \Delta(K_s * \chi_1))\|_1 + \lambda_2 \|M \circ (B - (K_s * \chi_1 + B_e))\|_2^2 + \lambda_3 \|M^C \circ (\chi_1 + \chi_0 / \delta)\|_2^2 \right]$$

Simultaneously estimating the external susceptibility outside the brain

### SSTV, SSTGV

Single Step QSM with Total Variation / Total Generalized Variation penalties

$$\min_{\chi} \frac{1}{2} \sum_i \left\| M_i F^{-1} H_i D F \chi - M_i F^{-1} H_i F \Psi(\phi) \right\|_2^2 + R(\chi)$$

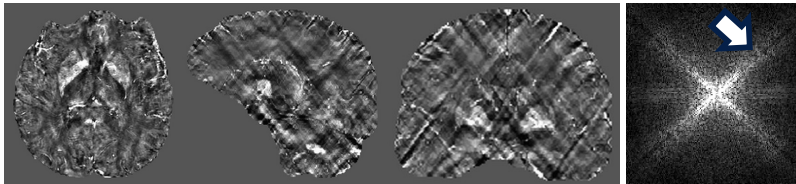
Perform VSHARP background field removal and dipole inversion in a single step



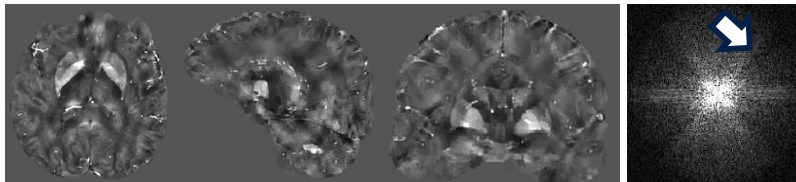
# QSM Dipole Inversion: iterative inversion methods with regularization

## Parameter optimization

(A)  $\lambda = 10^{-6}$



$\lambda = 10^{-4.2}$

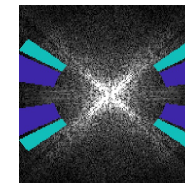
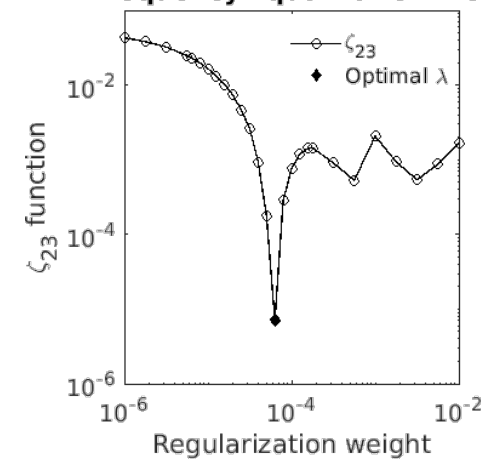


$\lambda = 10^{-3.5}$



(B)

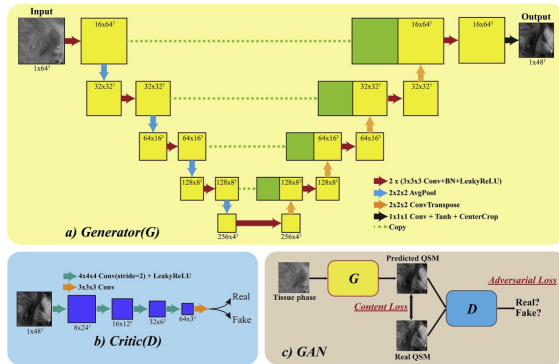
Frequency Equalization Plot



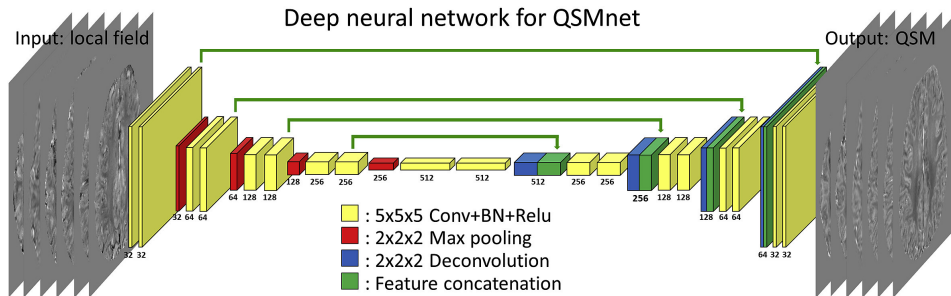
$\blacksquare$  M2  $\xi_{ij} = \left( \frac{A_i - A_j}{A_i + A_j} \right)^2$   
 $\blacksquare$  M3  $A_i$ : Mean power in  $M_i$

# QSM Dipole Inversion: deep learning-based methods

QSMGAN



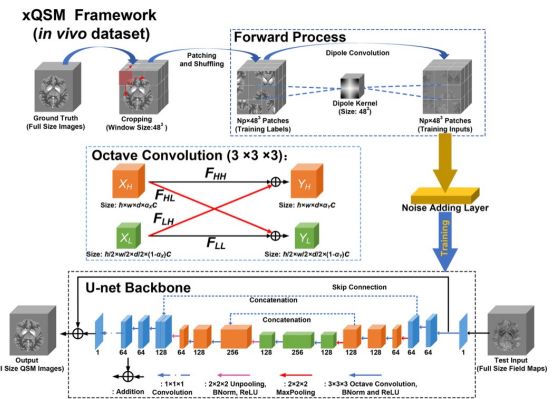
QSMnet+



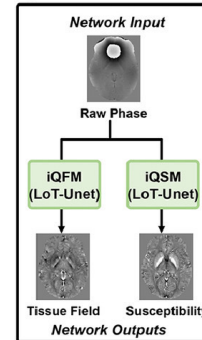
xQSM

Single step

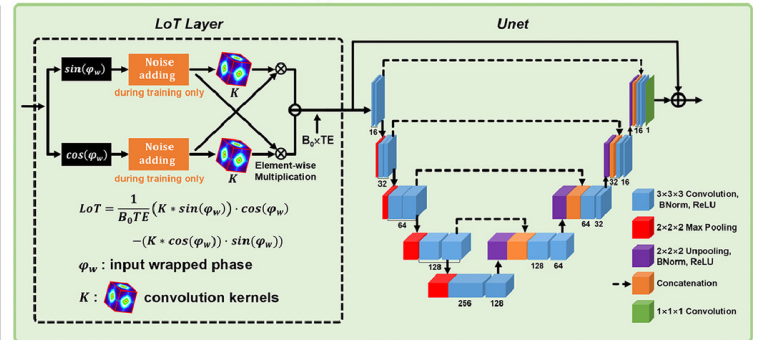
iQSM



(a) Overall Framework



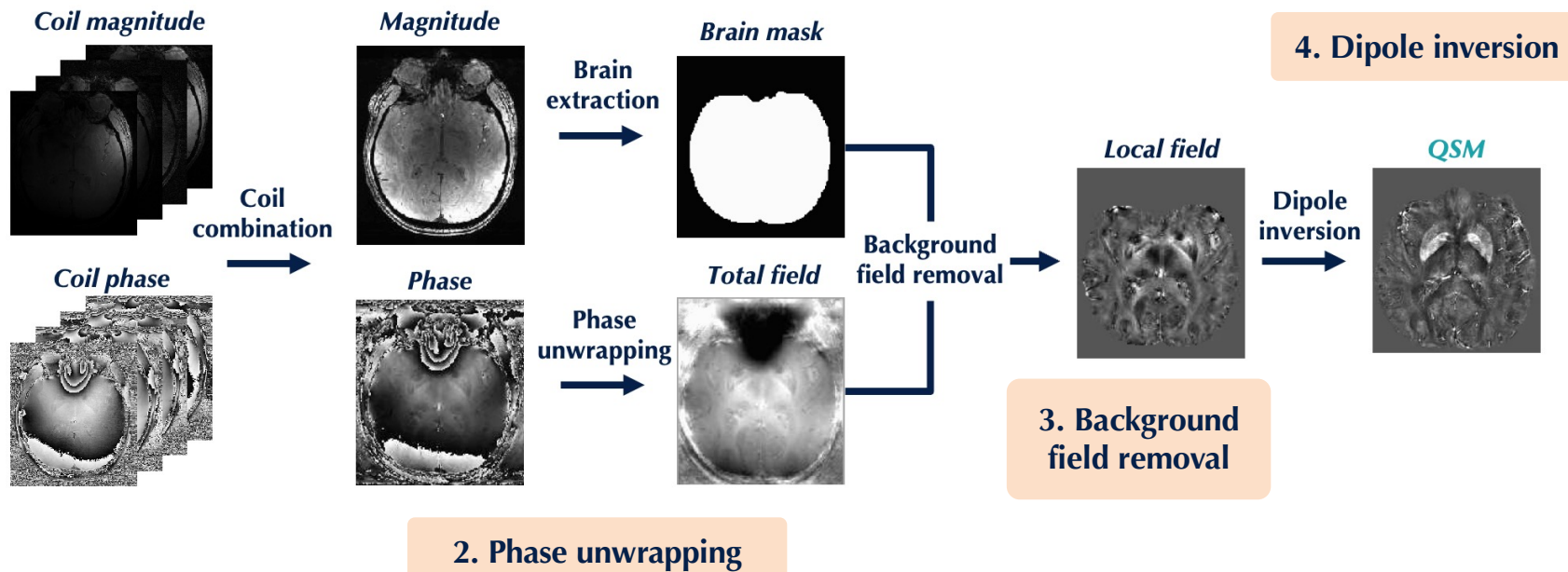
(b) LoT-Unet Architecture



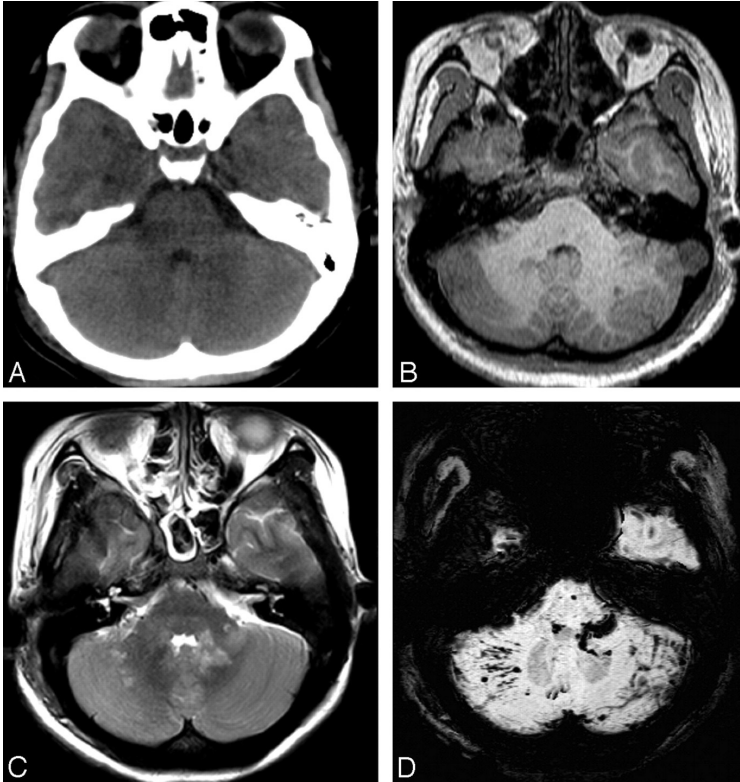
# QSM - Processing

## 1. Coil combination

$T_2^*$ -weighted sequence



## SWI – Traumatic brain injury



Iron

Blood product

Vascular abnormalities

Iron deposition

Calcium

Infection

Tumor

- SWI is **3–6 times more sensitive** than conventional  $T_2^*$ -weighted gradient-echo sequences in detecting the size, number, volume, and distribution of hemorrhagic lesions in DAI.
- Number and volume of SWI hemorrhagic lesions appear to **correlate with specific neuropsychological deficits**.
- Especially helpful in **detecting traumatic lesions in the brainstem**, whereas other MR imaging sequences have failed to detect structural abnormalities.

## SWI – Stroke

### Iron

Blood product

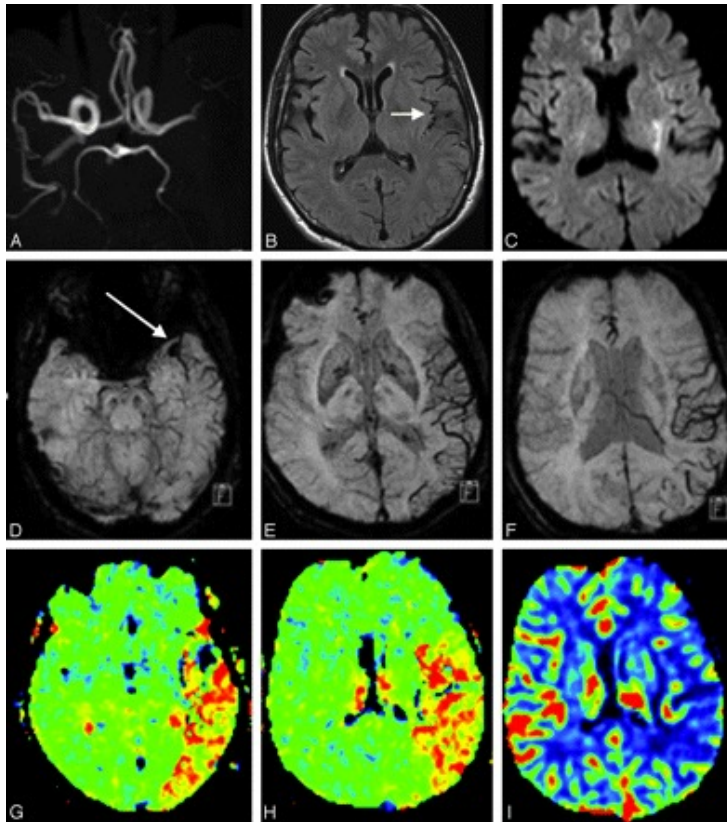
Vascular abnormalities

Iron deposition

### Calcium

Infection

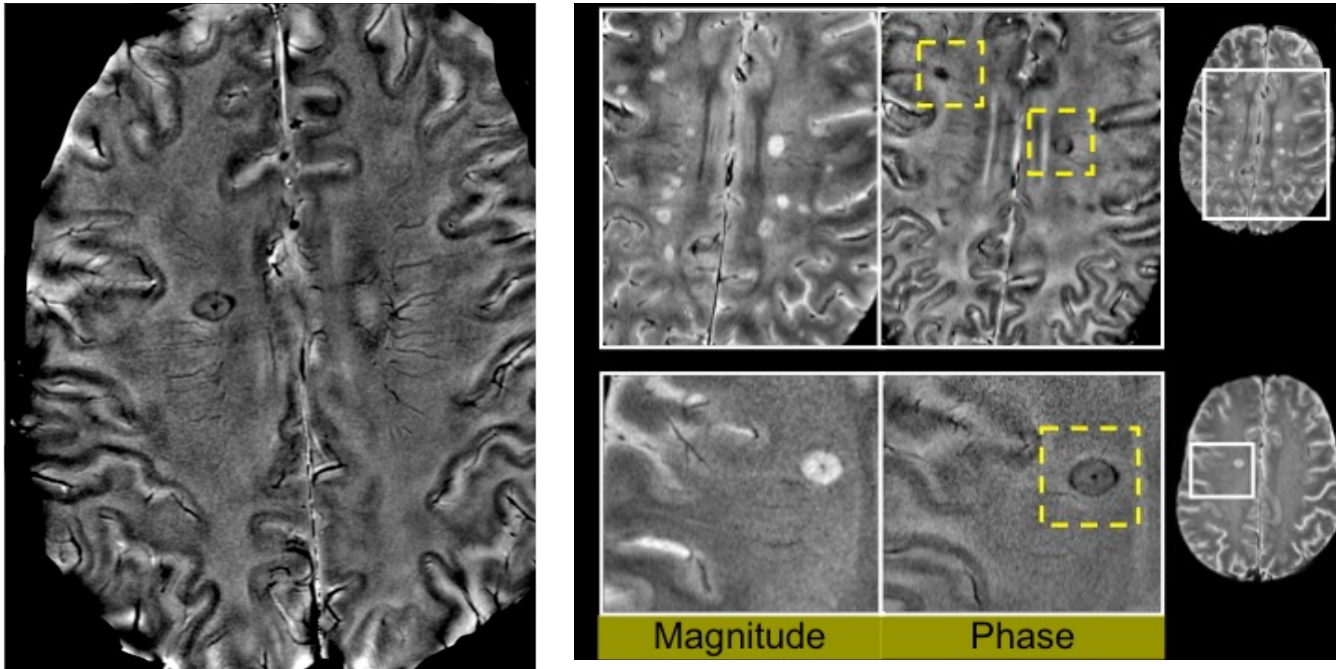
Tumor



- A 59-year-old man with a history of atrial fibrillation presented with sudden-onset right hemiparesis and speech deficits.
- MRI at 1.5T performed 2 hours after the onset of symptoms.
- SWI shows **prominent hypointense signals in the draining veins within areas of impaired perfusion.**



# SWI – Multiple Sclerosis



## Iron

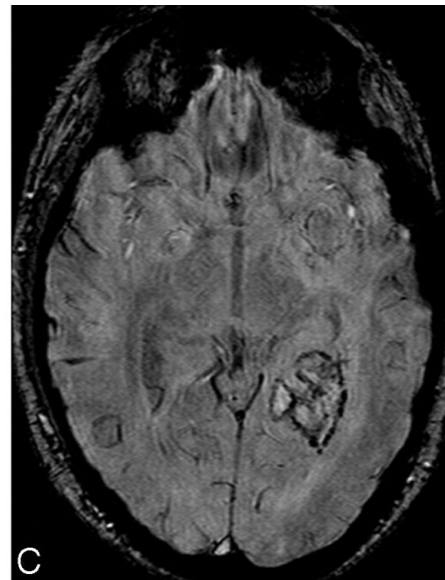
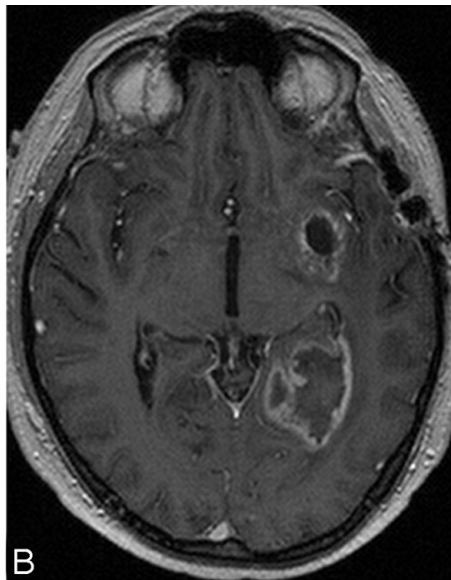
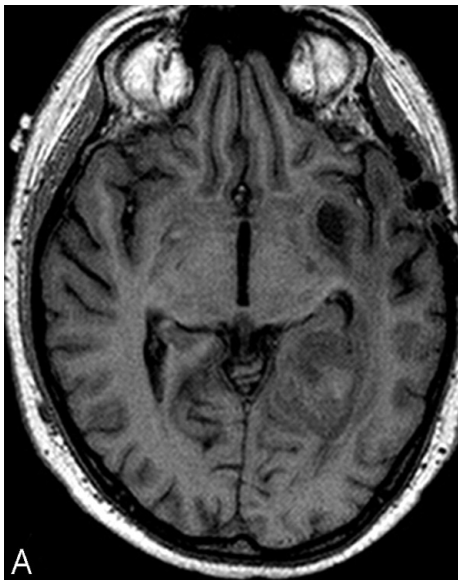
- Blood product
- Vascular abnormalities
- Iron deposition

## Calcium

- Infection
- Tumor

- Central vein sign
- Hypointense rim

## SWI – Brain tumors



### Iron

Blood product

Vascular abnormalities

Iron deposition

### Calcium

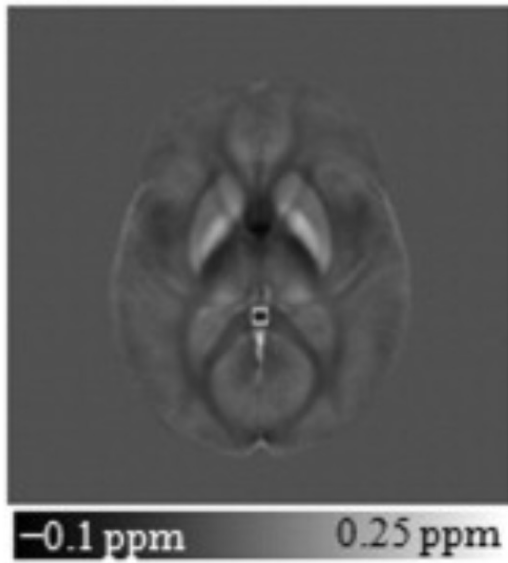
Infection

Tumor

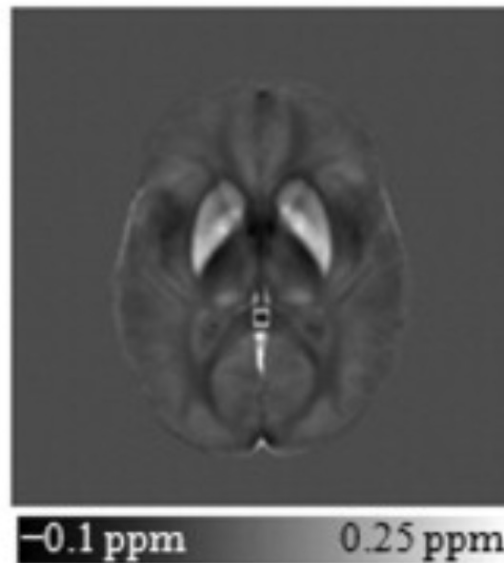
- Hemorrhage within tumors
- Pathologic vessels, angiogenesis



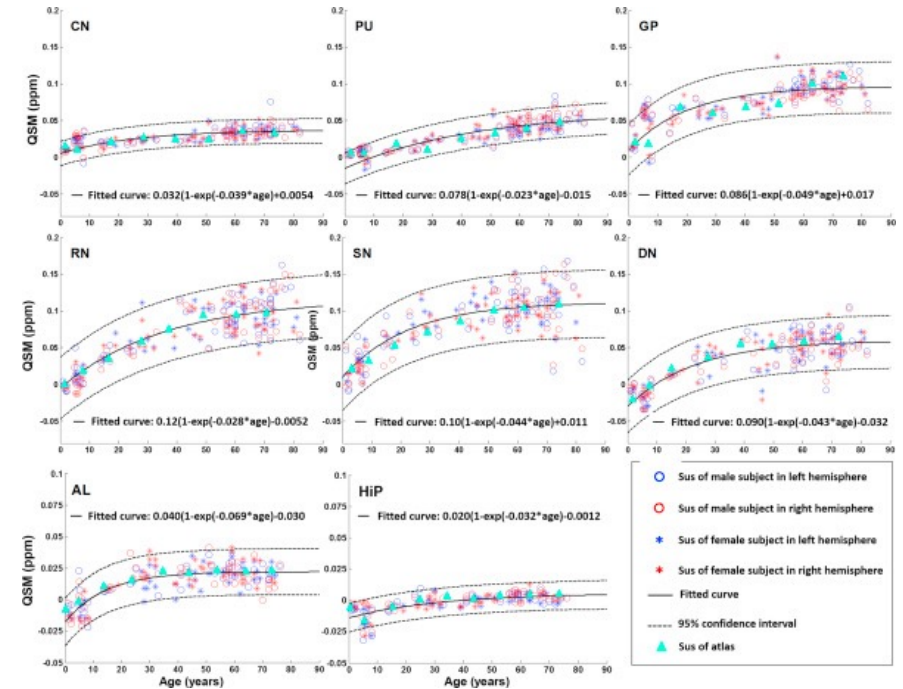
# QSM applications - Aging



Young

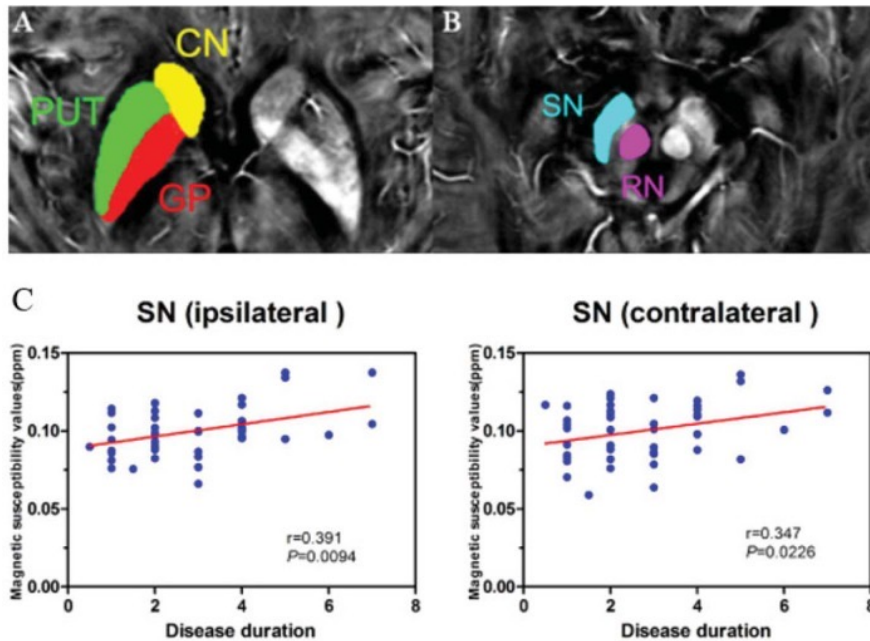


Elderly

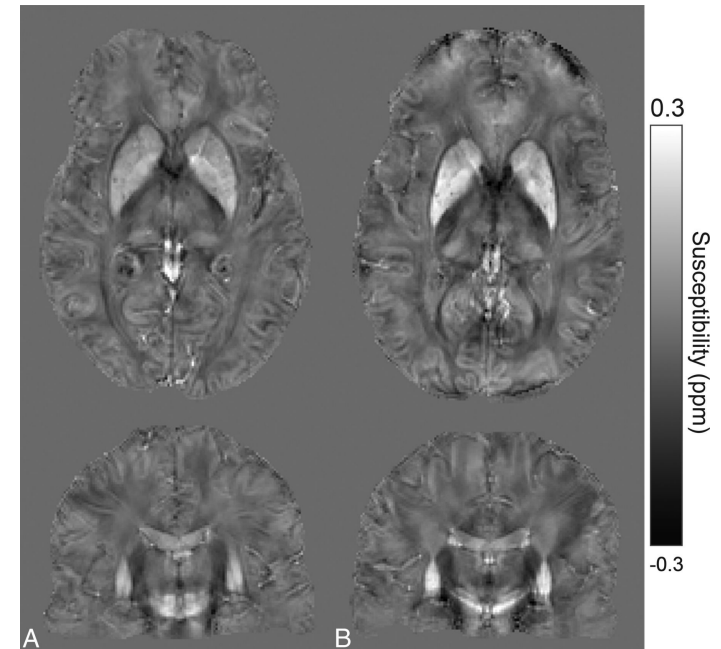


# QSM applications – Neurodegenerative diseases

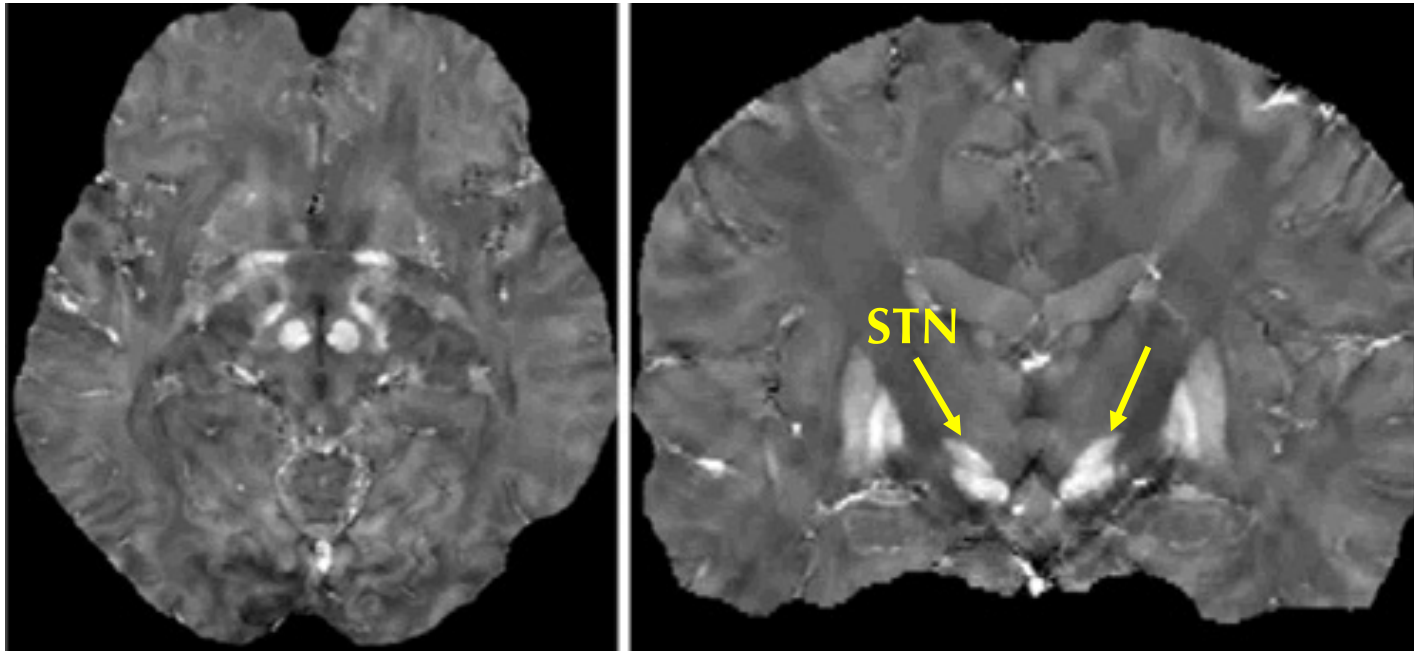
## Parkinson's Disease



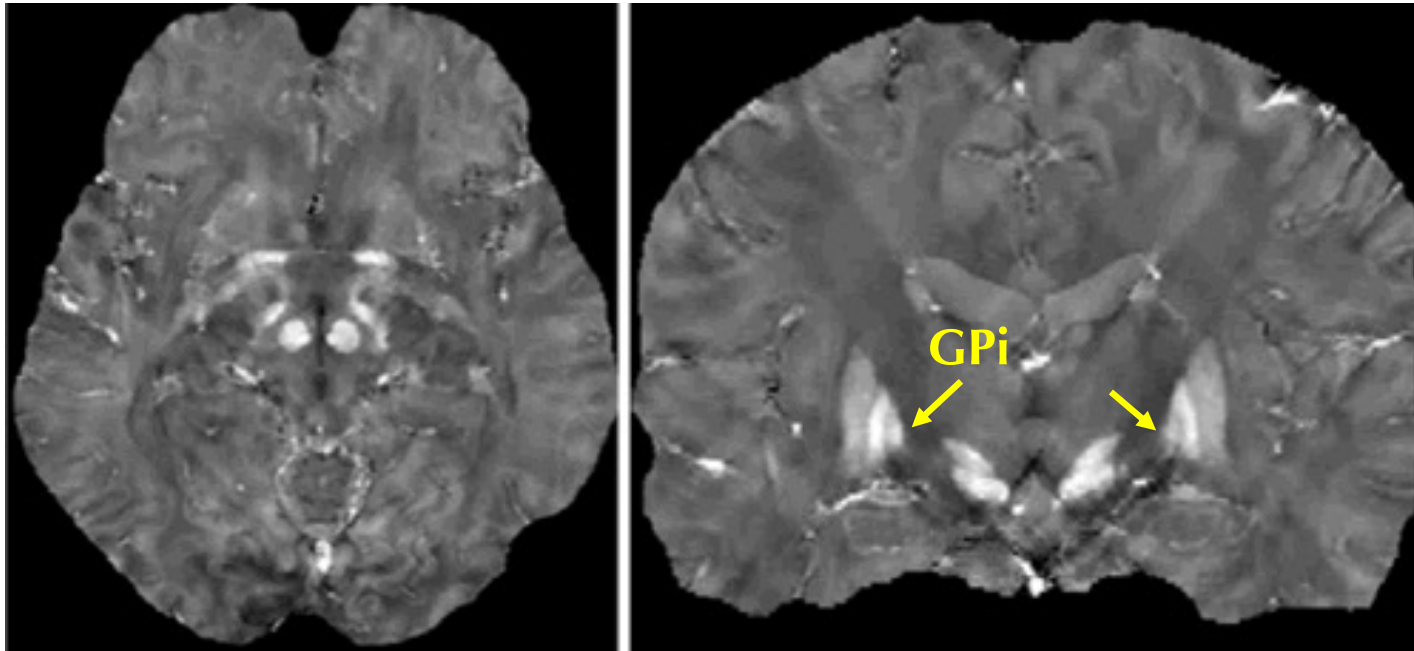
## Huntington's Disease



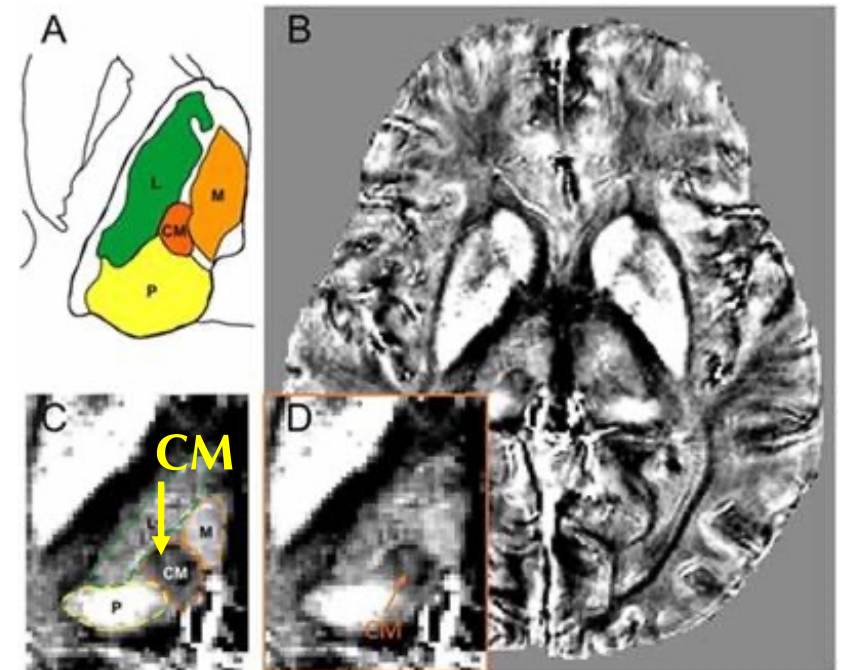
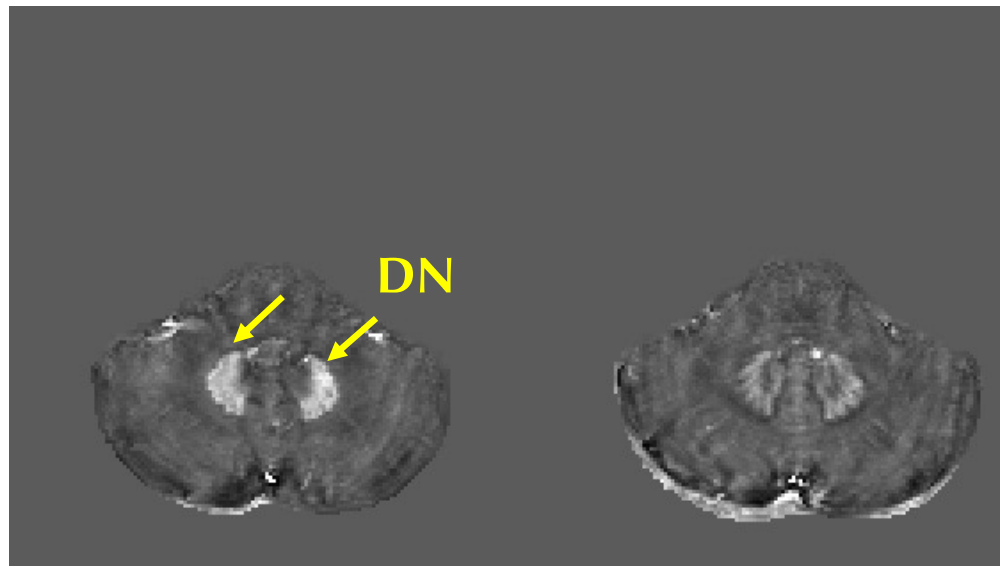
## QSM applications – Functional neurosurgery



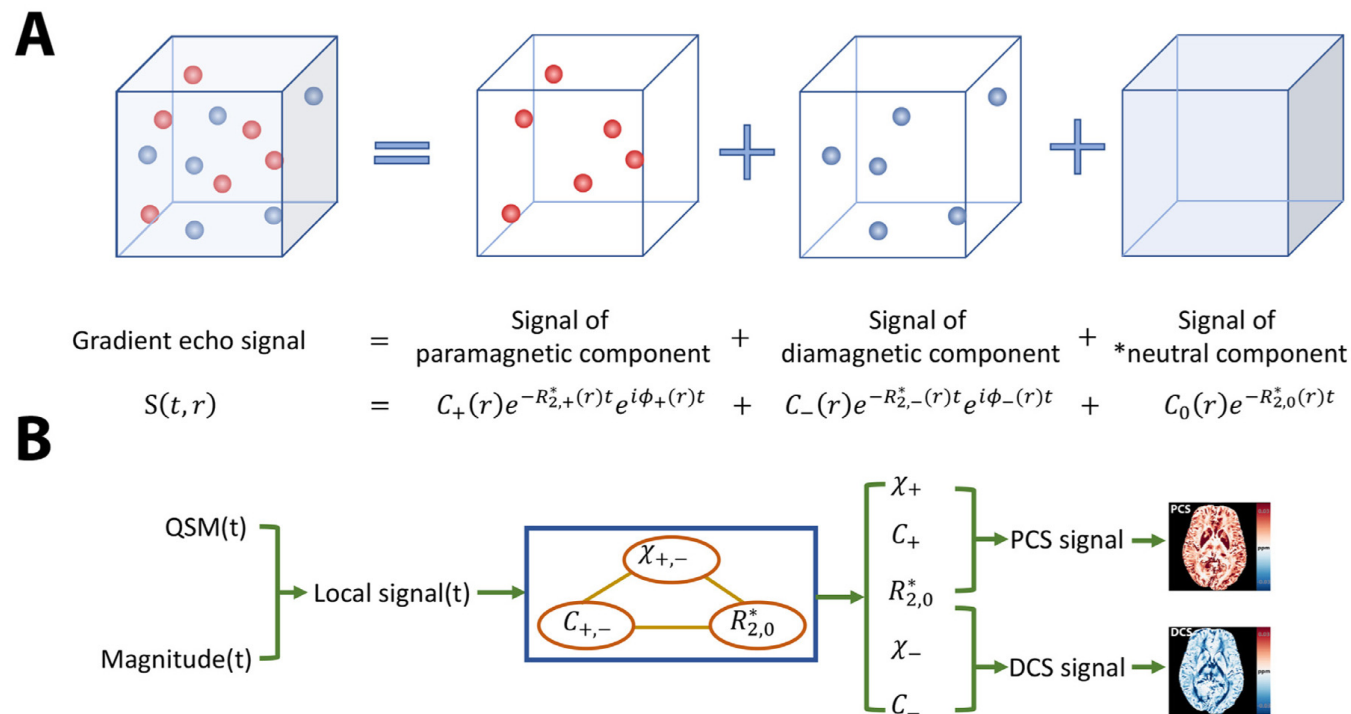
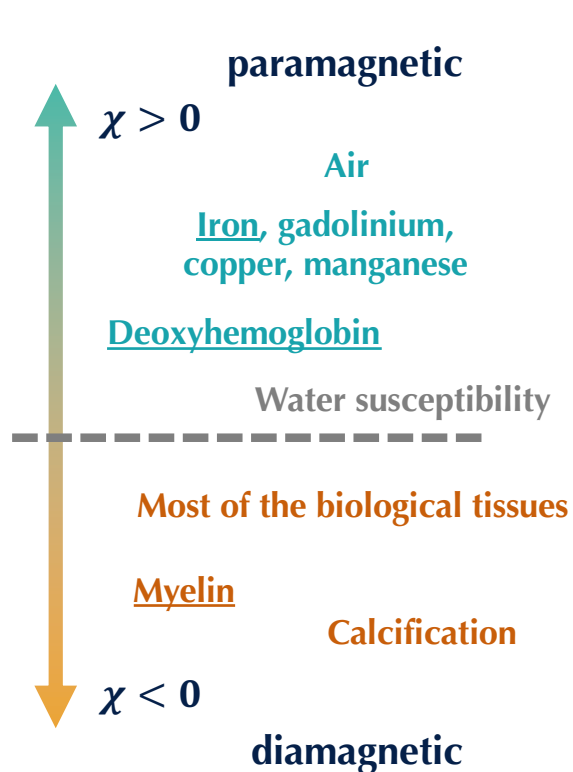
## QSM applications – Functional neurosurgery



## QSM applications – Functional neurosurgery



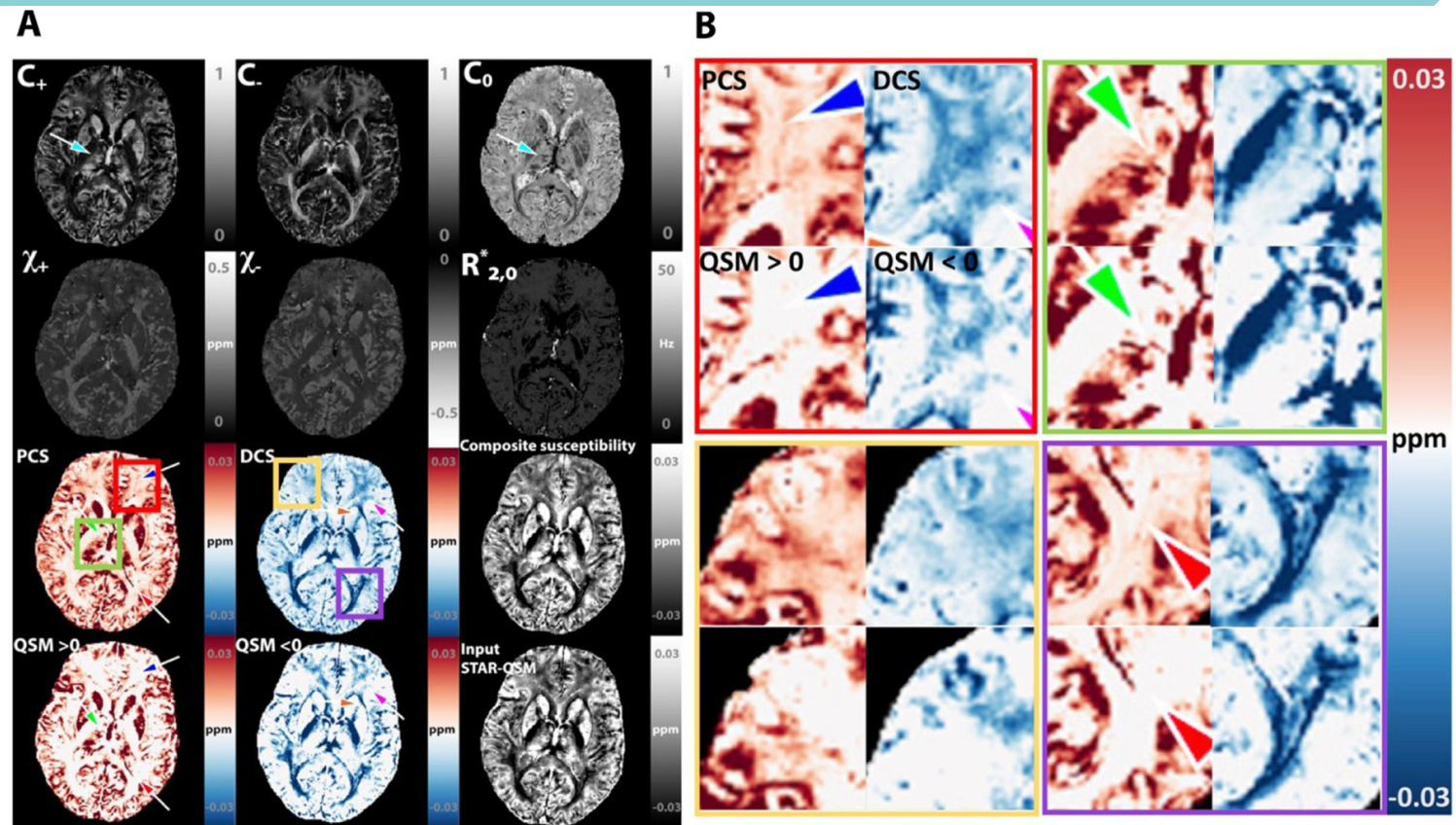
# QSM: Susceptibility source decomposition



\*neutral component means the component is susceptibility neutral relative to the susceptibility reference.



# QSM: Susceptibility source decomposition





# Summary

## Learning Objectives

- Explain the biological and physical basis of susceptibility effects in MRI.
- Interpret and process phase images for SWI.
- Understand the procedure of processing QSM.
- Recognize common applications of susceptibility imaging in neuroimaging.
- Appreciate the challenges and assumptions in going from phase to susceptibility maps.